

https://dspace.org/

On tin and lithium granite systems A crustal evolution perspective

N.J Gardiner; R.M Palin; L Koopmans; Laurence Robb

ELSEVIER SCIENCE BV
https://hdl.handle.net/10539/43593
WOS

Downloaded from a DSpace repository. https://dspace.org/

Earth-Science Reviews 258 (2024) 104947



Contents lists available at ScienceDirect

Earth-Science Reviews

journal homepage: www.elsevier.com/locate/earscirev



On tin and lithium granite systems: A crustal evolution perspective

Nicholas J. Gardiner [a,*], Richard M. Palin [b], Lot Koopmans [b], Martin F. Mangler [a], Laurence J. Robb [b,c]

[a] School of Earth and Environmental Sciences, University of St. Andrews, St. Andrews KT16 9AL, United Kingdom
[b] Department of Earth Sciences, University of Oxford, Oxford OX1 3AN, United Kingdom
[c] School of Geosciences, University of the Witwatersrand, Johannesburg, South Africa

ARTICLE INFO

Keywords:
Lithium
Tin
Tantalum
Tungsten
Pegmatite aplite spodumene petalite
U–Pb–Hf isotopes
Magmatism
Critical strategic battery metals

ABSTRACT

The battery metals tin and lithium (Sn—Li) are key to renewable energy technologies, with demand driving new interest in the formation and exploration of tin granites and lithium-caesium-tantalum (LCT) pegmatites. These magmatic-hydrothermal systems originate from highly evolved, reduced, peraluminous, volatile-rich granitic melts which develop elevated concentrations of incompatible metals. Tin granite deposits form either as disseminated magmatic cassiterite, or hydrothermal quartz-cassiterite lodes and greisens, with Li-bearing fluids driving late-stage mica alteration to Li-rich varieties. Conversely, LCT pegmatites record a complex crystallization with Li ores forming during primary magmatic crystallization, and Sn associated with hydrothermal overprints.

The first appearance in the geological record of Sn—Li granites and pegmatites is linked to the global onset of crustal reworking during Neoarchean terrane assembly, highlighting the key role of crustal evolution processes in their formation. In this contribution, we review our current understanding of Sn—Li metallogeny from source to sink through the lens of crustal processes. We focus on recent advances in petrological modelling and in situ microanalysis of rock-forming and accessory minerals, to examine tin granite and LCT pegmatite formation from partial melting of a source rock through melt extraction; emplacement, crystallization, and fractionation; to late-stage hydrothermal processes.

Quantitative thermodynamic modelling of crustal melting brings the ability to explore source rock anatexis and resulting melt compositions under various *P-T* conditions. Melt Sn—Li concentrations are controlled by mineral breakdown and metal partitioning between restite and melt. Sn and Li are primarily hosted in muscovite and biotite; deep crustal melting driving biotite breakdown releases Sn and Li into the melt, however shallow muscovite-driven melting restricts melt Li enrichment. It is difficult to generate a melt capable of saturating Li ore minerals from melting an ordinary clay protolith, hence either multi-stage melting or source metal pre-enrichment may be required.

Microanalysis allows high-precision geochemical and isotopic characterization of mineral phases. We review and summarize case studies using accessory minerals such as zircon, apatite, and mica, whose compositions are particularly powerful in tracking metal concentration and mobility during magma evolution and the magmatic-hydrothermal transition, with potential applications to exploration efforts. In tandem, the development of novel geochronometers such as cassiterite or columbite U—Pb help improve constraints on the age and timing of mineralization with respect to magmatism.

Finally, we consider the formation of tin granites and LCT pegmatites in 4D using the framework of long-lived, transcrustal magmatic systems. These models may help describe how prolonged melt generation, extraction, and evolution over protracted timescales allows progressive enrichment of Sn and Li. Combined, such efforts can help answer open questions on the formation of Sn—Li granite systems, to build improved 4D mineral systems models and inform fresh approaches to prospect for new deposits.

* Corresponding author.
E-mail address: nick.gardiner@st-andrews.ac.uk (N.J. Gardiner).

https://doi.org/10.1016/j.earscirev.2024.104947
Received 24 May 2024; Received in revised form 10 September 2024; Accepted 30 September 2024
Available online 5 October 2024
0012-8252/© 2024 The Authors. Published by Elsevier B.V. This is an open access article under the CC BY license (http://creativecommons.org/licenses/by/4.0/).

1. Introduction

"The earth does not conceal metals in her depths because she does not wish that men should dig them out, but because provident and sagacious Nature has appointed for each thing its place" Agricola, De Re Metallica, 1556 – translated by H. C. Hoover & L. H. Hoover, London, Mining Magazine, 1912.

Few magmatic rock types surpass granites in terms of the diversity of related mineral deposits (e.g., Černý et al., 2005). Specifically, S-type i.e. peraluminous granites formed from crustal melts host, or are associated with, major global deposits of the metals tin (Sn) and lithium (Li), as well as tungsten (W) and tantalum–niobium (Ta—Nb), all considered to be metals critical for renewable energy systems (Gardiner et al., 2024; IEA, 2022; US Geological Survey, 2023). The increasing demand for these metals reflects their central role in the electricity generation and storage technologies that enable energy decarbonization. This new demand has in turn driven a resurgence of interest in the formation of both tin granites and metalliferous or rare-metal pegmatites.

The term 'tin granite' typically describes Sn-bearing granitic bodies and related minor intrusions (e.g., Lehmann, 1990), some of which may also contain Li. Likewise, typical primary hard-rock Li deposits are associated with lithium–caesium–tantalum (LCT)-type pegmatites (Černý, 1992; Linnen et al., 2012; London, 2008), minor but exotic granitic intrusions formed from highly fractionated volatile-rich peraluminous melts (Černý, 1991a). Many LCT pegmatites are also Sn-bearing, for which they were originally exploited (Partington, 2017). However, granite-hosted Sn and Li deposits are relatively uncommon, tending to have formed in metallogenic provinces specific in terms of their secular distribution, tectonic setting, and metal endowment (McCauley and Bradley, 2014; Romer and Kroner, 2016; Tkachev, 2011).

Fundamentally, the formation of granite-related Sn and Li deposits requires geological processes that concentrate these typically trace metals within a silica-rich melt to such significant degrees that they either: (i) act as major elements, thereby saturating ore and/or rock-forming minerals such as the Sn oxide cassiterite and the Li aluminosilicates spodumene and petalite; and/or (ii) are available in sufficient quantities that these fluid-mobile metals may be efficiently extracted by magmatic-hydrothermal fluids during vapour saturation (Burnham, 1979) to precipitate hydrothermal ore minerals. Under typical conditions, the formation of ore minerals requires melt metal concentrations that exceed ordinary mid-upper crustal abundances by at least one order of magnitude (e.g., for Sn 10-20×), although potentially much more. Spodumene saturation requires a granitic melt to reach Li concentrations of at least 5000 ppm (London, 1984; Maneta et al., 2015), representing an enrichment of ca. 250 times average crustal abundances (Rudnick and Gao, 2014). Therefore, to build metallogenic models for these deposits, we must constrain how metals are retained and concentrated within a dynamically evolving granitic system.

Granites form by the sequential partial melting of a source rock, the extraction of that melt, and then its emplacement, assimilation, and accompanying fractional crystallization during cooling, ultimately leading to vapour saturation – i.e. the magmatic-hydrothermal transition. These processes concentrate incompatible metals and hence are the primary driving forces for the long-term evolution and differentiation of Earth's continental crust. Much geochemical and isotopic work on tin granites and LCT pegmatites has been traditionally undertaken from a whole-rock perspective (e.g., Lehmann, 1990 and refs therein). However, the recent development of new analytical and modelling tools has the potential to significantly advance our understanding of such crustal evolution processes.

Firstly, advances in chemical microanalysis allows high-precision in situ geochemical, geochronological, and isotopic characterization of mineral phases, notably of zoned accessory minerals such as zircon and apatite (Bruand et al., 2020; Kemp and Hawkesworth, 2014). Mineral-based tools are more robust recorders of melt chemistry than whole-rock; for example, minerals may saturate early and then progressively during crystallization and thus provide time-integrated records of magmatic processes. Further, as many granites are the products of crustal storage and reworking, the ability to analyze inherited mineral domains yields information on granite prehistory which is lost from the bulk geochemical record. A recent advance is the analysis of mineral metal contents that now have the potential to be used as tracers of metallogenesis (e.g., Gardiner et al., 2021; Guo et al., 2022; Li et al., 2022; Mangler et al., 2024).

Secondly, improvements to equilibrium thermodynamics-based models have recently expanded a traditionally sub-solidus metamorphic toolkit into the supra-solidus realm, allowing the calculation of stable phase assemblages plus melt, and the ability to explore melt compositions at different physico-chemical conditions (e.g., *P, T,* X_{H2O}) (Green et al., 2016; White et al., 2014). This toolkit facilitates development of a quantitative understanding of the processes of crustal melting (anatexis) and allows tighter constraints of the conditions and nature of melting, such as crustal depth and water activity, as well as the role of restitic minerals in melt metal budgets. These methods can therefore predict how granitic melts become endowed with metals during crustal anatexis.

Finally, the development of new mineral-based geochronometers and tracers allows high-precision dating of mineralizing systems, either of hard-to-date host rocks, or the ore mineral directly. Such chronometers include cassiterite U—Pb and mica Rb—Sr (Tapster and Bright, 2020; Zack and Hogmalm, 2016), which have the potential to shed new light on understanding the timescales of mineralizing systems and their relationship to 4D magmatic evolution.

In this contribution we review our current understanding of Sn—Li granite systems from source to sink via the use of these novel analytical and modelling tools. Since Sn and Li deposits are genetically related, we consider them together to build holistic knowledge. We focus on recent case studies to highlight the potential of mineral-based analytical and numerical approaches to better constrain the processes that concentrate these economically important metals in granitic melts; to build 4D petrological models of these systems; and to develop potential 'pathfinders' to discover new deposits. We conclude by identifying future research directions in deploying new mineral-based tools and modelling approaches.

2. The energy transition and the role of tin and lithium

The transition to a renewable energy platform, at the heart of efforts to reach net zero carbon emissions by 2050 or earlier, will only be made possible by a significant and rapid sourcing of sufficient quantities of strategic 'battery' metals (Gardiner et al., 2023b; IEA, 2022; Jowitt and McNulty, 2021), marking a fundamental shift in the resource basis of society. At present, this demand for metals will only be met by ongoing and enhanced sourcing from both new and existing mines, ideally with a smaller environmental footprint than in the past (Smith and Wentworth, 2022). Some of these battery metals such as Sn and Li are considered critical, having both economic and industrial importance resulting in growing demand combined with insecure supply chains (McNulty and Jowitt, 2021). Lithium is a core component of Li-ion batteries, whilst due to its low melting point, Sn is a fundamental constituent in modern electrical solders.

Tin and lithium are metals mined at small-scale with mined tonnages ca. 100× less than for example copper (US Geological Survey, 2023). Such small mined tonnage metals suffer from price and supply volatility (Redlinger and Eggert, 2016), with historically low demand and variably immature markets now experiencing a significant uptick due to their use in new technologies. Global demand for Li in particular is soaring, with current supply now dominated by pegmatite-sourced lithium hydroxide (Gardiner et al., 2024). Many economic Li-bearing pegmatites were historically mined for Sn and Cs, with Li as a by-product, and are being re-opened as brownfields projects. However,

there is now increasing interest in greenfields Li exploration (Phelps-Barber et al., 2022). In comparison, Sn has been historically mined for centuries (Agricola, 1556). However, the 1986 collapse of the International Tin Council heralded the decline of Sn exploration and production, leading to the closure of many tin mines globally; it was only in the 2000's that the development of Sn as a substitute for lead in electrical solder reignited such demand that mine supply was initially unable to keep up (Gardiner et al., 2015b). The development of new technologies (e.g., renewable energy, robotics, artificial intelligence and supercomputing) all of which require Sn in significant quantities means it is the 'metal that glues the technological revolution' (Rio Tinto and Latham, 2018). Thus, a key research goal is to make both Sn and Li sustainable, achieved by enabling the discovery, extraction and (re) processing of more metals and by broadening the supply chain.

3. Tin and lithium granites and pegmatites

3.1. Overview

The term "tin granite" was first coined by Humboldt (1823), who in accord with his neptunist view of magmatism at the time, described "*granite stannifère vs granite primitif*", namely tin-bearing versus primitive (barren) granite deposited during different epochs. Barsukov (1957) more specifically described tin granites as those "*characterized by higher tin contents in those varieties that have not been altered by contact or post-magmatic processes*", and subsequently expanded this definition to require tin contents of up to "*4 to 5 times the Clarke of tin*" (i.e. 16–30 ppm). However, as pointed out by Lehmann (2021), any definition of tin granites is somewhat arbitrary, since the mineralized phases are typically part of much larger magmatic systems. Tin granite research reached its apogee in the 1960s to 1980s (Barsukov, 1957; Heinrich, 1990; Lehmann, 1982; Mitchell, 1977; Schuiling, 1967; Taylor, 1979), but scientific interest then waned as metal demand declined in the 1990s.

In parallel, interest in granitic pegmatites grew rapidly during the 19th century, with geologists offering a multitude of theories on their petrogenesis and internal processes by the middle of the 20th century (Cameron et al., 1949; Jahns, 1955). Due to their textural and mineralogical complexity, providing a general definition of pegmatites remains controversial, with most researchers agreeing on "*an essentially igneous rock that is distinguished from other igneous rocks by its extremely coarse but variable grain size, or by an abundance of crystals with skeletal, graphic, or other strongly directional growth habits*" (London, 2008). Subsequent work on pegmatites has focused on understanding their source and defining classification schemes (Černý, 1991b; Černý, 1991a), leading to a geochemical discrimination between lithium–caesium–tantalum (LCT)– and niobium–yttrium–fluorine (NYF)–type pegmatites based on their differing source and genetic conditions.

Our present-day understanding of Sn and Li-bearing granites and pegmatites is that they form from highly evolved peraluminous silicic melts, which develop high concentrations of both incompatible metals (e.g., Be, Ta, In, Sb, Bi; (Simons et al., 2017; Taylor, 1979)) and volatile phases (e.g., H_2O, Cl, F, and B (Manning and Exley, 1984)) during the final stages of magmatic crystallization, as evidenced by the common association with tourmaline and fluorite. LCT pegmatite bulk compositions are close to that of a granite, approximating granitic minimum melts, with formation temperatures approximately 400–600 °C (Troch et al., 2022). The fundamental rock-forming assemblage for both tin granites and LCT pegmatites is simple, consisting of varying proportions of potassic feldspar, albite, quartz, and a minor amount of muscovite and/or biotite.

3.2. Geodynamic framework

Evolving geodynamics and accompanying changes in tectonic regimes are key to the formation of many mineral deposits (Groves and Bierlein, 2007; Kerrich et al., 2005; Mitchell and Garson, 1981). Geodynamic processes provide essential sources of energy into mineral systems at lithospheric scales, heat, and fluids, and serve to juxtapose rock units. This highlights the need to develop 4D metallogenic models for typically transient ore formation within much longer-lived geodynamics, to inform on exploration strategies up to the scale of continents.

Tin provinces are the classic metallotect (Lehmann, 1990; Werner, 1791). They typically result from long-lived plate margin processes (see Section 3.3), in some cases forming metal-fertile regions stretching hundreds to thousands of km, such as the Bolivian tin belt and the Southeast Asian granite belts of Myanmar, Malaysia, and Thailand. Within these regions, multiple episodes of granitic magmatism are recorded, some of which are associated with Sn and/or Li mineralization. Individual episodes typically last on the order of less than a few Myr, but together they reflect long-lived, crustal evolution over tens to hundreds of Myr (Cobbing et al., 1986; Gardiner et al., 2018; McBride et al., 1983). The classic view is that these magmatic events over time form large composite intrusions, described as batholithic in form, as exemplified by the Lachlan S-type granites in Australia (Chappell and White, 2001) and the Cornubian granites of Southwest England (Floyd et al., 1993). Discrete granitic intrusion episodes were thought to represent successive extractions from a common melt source (e.g., Simons et al., 2016). Upon extraction, these intrusions undergo further cooling and accompanying fractional crystallization and vapour saturation. However, not every phase of magmatism necessarily leads to related mineralization. As an example, the Cornubian batholith developed over a period of some 25 Myr, with the latest classification defining five main granitic suites of which only 2–3 are considered mineralized (Simons et al., 2016).

This traditional batholithic view of granitic systems is now coming under reassessment. There is an increasing recognition that many magmatic systems are not only long-lived but are vertically extensive, accompanied by a changing view of magma chambers from that of being melt-dominated and vigorously convecting, to crystal-dominated ('mush') and conductively cooled (e.g., Bachmann and Bergantz, 2004). Plumbing systems feeding volcanoes are now referred to as 'transcrustal' magmatic systems (Cashman et al., 2017), and while not all granites with a crustal source are necessarily fuelled by mantle-derived magmatic inputs into the lower crust, the concept of extensive crustal mush systems is a useful lens through which to view Sn—Li magmatism (Fig. 1). For example, small-volume discrete granitic extractions on the scale of 10's m (i.e. pegmatite bodies) to 10's kms may represent the upper crustal parts of a much larger system, periodically tapped from crystal-rich mushes and ephemeral melt lenses ponding in the mid crust, and a lower crustal supply of heat and potentially melt and volatiles. These magma reservoirs evolve via low-degree buoyant reactive melt flow maintaining local equilibrium but driving broader scale chemical gradients and differentiation (Edmonds et al., 2019; Jackson et al., 2018).

While the transcrustal or whole-lithosphere concept was originally developed for arc-type systems and has recently been reviewed with respect to copper porphyry deposits (e.g., Chelle-Michou and Rottier, 2021), there is now an opportunity to explore the relevance of this model in terms of crustal melts and related Sn—Li deposits (e.g., Bi et al., 2024; Edmonds et al., 2019; Lehmann, 2021). This view must accommodate the drivers for crustal melting which may be varied - including orogeny, and post-orogenic collapse and crustal extension – plus a mix of possible sources of melt and of heat and fluids, including mid-crustal metasedimentary material and/or a role for mantle melting; all of which underpin a broad, deep and long-lived melt zone. The transcrustal magmatic view highlights the importance of timescales in understanding such systems, as they develop over tens of millions of years in tectonic systems that are themselves continually evolving, but which may manifest discrete, punctuated mineralization events.

The origin and role of pegmatites within a whole-lithosphere or

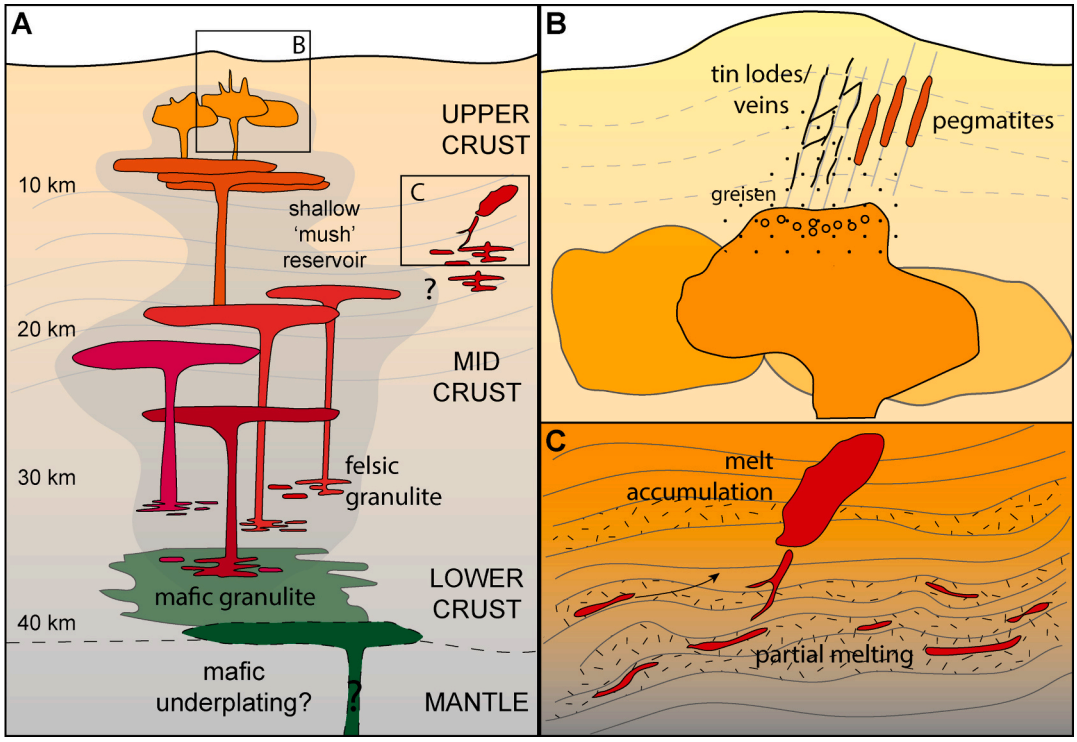


Fig. 1. A. Whole-lithosphere or 'transcrustal' system for Sn—Li magmatism and mineralization, after Cashman et al. (2017). In this model, a long-lived vertically-extensive crystal mush dominated magmatic system leads to stages of magmatic evolution, culminating in Sn—Li rich magmas ponding in the upper crust. B. Close-up of upper-crustal tin granite, with related Sn hydrothermal system (lodes, veins and greisens) and LCT pegmatites as minor melt extractions; after Černý et al. (2005). C. Anatectic LCT pegmatite formation from partial melting of metasedimentary crust and ensuing melt accumulation, after Koopmans et al. (2023).

transcrustal magmatic framework remains a matter of debate. By contrast to tin granites, LCT pegmatites are typically very small bodies, mostly measuring 10–100's m in length, and which crystallize rapidly from their incipient melt (Černý, 1991b). These pegmatites commonly form in groups, sometimes with more than 1000 individual intrusions situated within a few tens of km^2, and they are typically spatially and temporally associated with syn- to late-orogenic magmatic suites. Some pegmatite groups (fields) exhibit regional zonation transitioning from barren to progressively more evolved and incompatible-rich bodies (Černý, 1991a; Černý, 1991b). Although many are correlated to particular granitic bodies, this does not necessarily imply that all LCT pegmatites are derived from highly fractionated granitic intrusions: an alternative view suggests that LCT pegmatites may result from small-degree anatectic melts (Fig. 1c) (Koopmans et al., 2023; Müller et al., 2017; Shaw et al., 2022; Shaw et al., 2016; Simmons et al., 1995; Stewart, 1978). These end-member scenarios are discussed in more detail below.

3.3. Tectonic settings

Tin and Li provinces form in both orogenic belts and anorogenic settings. Geodynamic environments that promote granitoid magmatism and associated mineralization are typically:

(i) accretionary margins, such as the classic tin belts of South America and the Western and Eastern belts of Southeast Asia which formed adjacent to, albeit inboard of, long-lived subduction zones (Cobbing et al., 1986; Hutchison, 1977; Searle et al., 2012);

(ii) (post)collisional orogenic settings as typified by the tin granites of the European Variscan orogeny and best seen in Southwest England, Brittany, the Erzgebirge in Germany and the Czech Republic (Marignac and Cuney, 1999, p. 199); and by LCT pegmatites in continent-continent collisional zones, such as the Sn-bearing Kamativi pegmatite in Zimbabwe (Shaw et al., 2022); and the Pan-African Damara pegmatite belts in Namibia (Fuchsloch et al., 2018);

(iii) anorogenic intra-cratonic settings such as the A-type granites of the Bushveld and the Jos plateau in Nigeria (Kinnaird and Bowden, 1987; Robb et al., 2000);

and

(iv) late Archean geodynamic settings, typically where Archean tonalite-trondhjemite-granodiorite (TTG) terranes experienced Meso-Neoarchean crustal maturation such as the ca. 2.8–2.7 Ga tin granites and pegmatites of the Kaapvaal and Pilbara Cratons (Sweetapple and Collins, 2002; Trumbull, 1993), and the ca. 2.6 Ga LCT pegmatites found in the greenstone belts of Zimbabwe and Manitoba (Dittrich et al., 2019a, 2019b; Stilling et al., 2006).

3.3.1. Secular distribution

The global distribution of Sn and Li granites and LCT pegmatites points towards a clustering in space and time. A significant proportion (~90 %) of current Sn resources, as well as historical global production, comes from three main regions: the Tethyan-related granite belts of Southeast Asia, the Eastern Cordillera of the Central Andes (Bolivia and Peru), and the European Variscan granites (Schwartz et al., 1995). These provinces all formed from the Late Paleozoic through the Mesozoic into the early Cenozoic, and are genetically associated with active tectonic margins. The strong skew of such deposits towards the Phanerozoic may be a reflection of the inherently poor preservation potential of such provinces, in that shallow ore deposits formed on or adjacent to plate margins are susceptible to removal from the geologic record – either via erosion or through destructive margin processes (Cawood et al., 2013).

Less common are older Sn deposits, many of which are largely Proterozoic in age, and formed in relatively stable anorogenic, cratonic settings, such as Central Africa, South Africa, and Brazil (Kinnaird et al., 2016). However, significant historic Sn production has come from LCT pegmatites, for example Kamativi and the Greenbushes pegmatite in Western Australia, both now being explored and/or mined for Li.

LCT pegmatites in particular show distinct patterns in terms of their secular and geographic distribution. They first appeared in the geological record during the late Archean (ca. 3.2–2.5 Ga) (McCauley and Bradley, 2014), with examples documented in most cratons worldwide: the Yilgarn and Pilbara cratons, Western Australia (Jacobson, 2007; Sweetapple, 2017a, 2017b); the Zimbabwe and Kaapvaal cratons in southern Africa (Dittrich et al., 2019a, 2019b; Robb and Robb, 1986; Trumbull, 1993); and the Superior Craton in North America (Stilling et al., 2006). However, younger deposits are also found, with the pattern of LCT pegmatite formation ages reflecting orogenic cycles through time (Tkachev, 2011). Pegmatite age peaks at ca. 2.65, 1.8, 0.5 and 0.35 Ga may thus reflect supercontinent assembly (McCauley and Bradley, 2014).

3.3.2. *Late Archean Sn—Li granites*

Perhaps the oldest dated Sn and Li deposits are found associated with the Sinceni Pluton of ESwatini (Swaziland) in the eastern Kaapvaal Craton. Rb—Sr dating of the main pluton and co-genetic LCT pegmatites has yielded ages of ca. 3.0 Ga (Trumbull, 1993), while cassiterite has yielded a U—Pb age of 3086 Ma (Leopardi et al., 2024). Other contenders for the oldest recorded LCT pegmatite include the 2829 Ma Wodgina pegmatite in the Pilbara Craton (Kinny, 2000), and a reported garnet Pb—Pb age of 2912 Ma from the Union pegmatite in the Murchison Greenstone Belt, also from the Kaapvaal Craton (Kruger et al., 1998; Robb and Robb, 1986).

The appearance of such mineralized granites in the late Archean reflects a profound shift in Earth geodynamics. Archean craton development involves the protracted formation of juvenile continental (TTG) terranes, typically during the early Archean (4.0–3.2 Ma). These terranes were then assembled, thickened, and stabilized during the late Archean to form cratons, an assembly linked to the onset of horizontal plate tectonics (Brown et al., 2020; Cawood et al., 2018; Gardiner et al., 2023a). This period of cratonisation is also marked by the first appearance globally of potassic granites *sensu stricto*, and of economic LCT pegmatites, reflecting the onset of widespread crustal reworking (Cawood et al., 2018; Kendall-Langley et al., 2020; Laurent et al., 2014). This temporal and in some cases genetic relationship between LCT pegmatites and potassic granites is observed in many cratons (Fig. 2). For example, the significant LCT pegmatites of: Bikita in the Zimbabwe Craton (2616 Ma; Melcher et al. (2015)), Tanco in the Superior Craton (2641 Ma; Camacho et al. (2012)) and the Mount Edgar pegmatites in the Pilbara (ca. 2850 Ma; Sweetapple and Collins (2002)) are all coincidental with the cratonic onset of granitic magmatism. However, whilst granites can be reliably dated using zircon U—Pb, constraining the age of pegmatites can be significantly more challenging. Issues of hydrothermal overprinting, highly metamict zircon, or usage of mineral

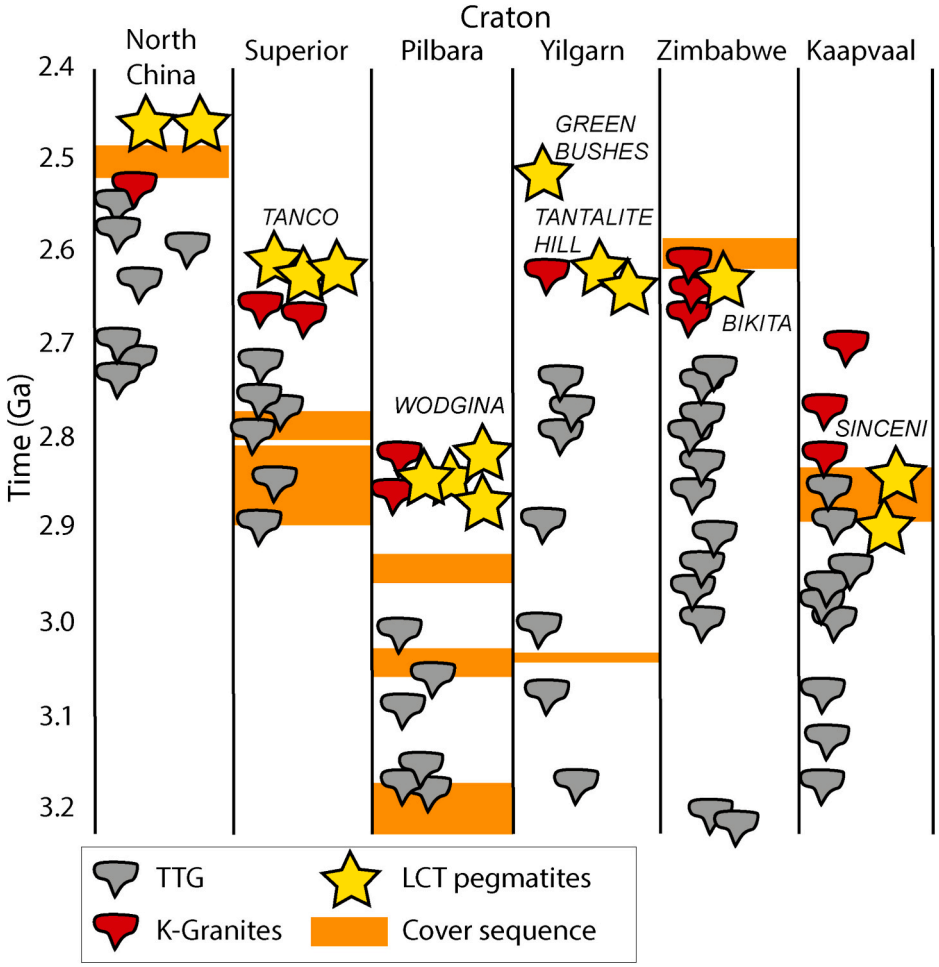


Fig. 2. Time-space plot for the North China, Superior, Pilbara, Yilgarn, Zimbabwe and Kaapvaal cratons for the period 3.2–2.4 Ga, showing the timing of formation of selected LCT pegmatites, TTG and late Archean granites. Also shown are age constraints of major sedimentary cover sequences, a proxy for crustal stabilization. After Cawood et al. (2018) and Gardiner et al. (2023a).

phases with significant initial Pb all complicate efforts to produce reliable ages with reasonable uncertainties. This is further discussed in the geochronology section.

Perhaps the world's most productive Li pegmatite province is the Yilgarn Craton, Western Australia, hosting at least 125 reported LCT pegmatites which together constitute the world's largest reserves of Li (Bowell et al., 2020), as well as significant Sn and Ta. The majority of the volumetrically significant Yilgarn pegmatites are hosted by mafic to ultramafic volcanic and volcano-sedimentary greenstone successions (Dittrich et al., 2019a, 2019b), rather than the granitoid basement. Reported ages of pegmatite crystallization of 2640–2620 Ma coincide with the final stages of deformation, cratonisation, and the emplacement of low-Ca granitoids (Mole et al., 2019), and include Greenbushes dated at 2527 Ma via U—Pb in both zircon and cassiterite (Kendall-Langley et al., 2020; Partington, 2017).

3.4. Styles of mineralization

The primary Sn and Li ore minerals are oxides or aluminosilicates. The main ore of Sn is cassiterite (SnO_2). Common Li ore minerals include the aluminosilicates spodumene ($LiAl(SiO_3)_2$) and petalite ($LiAlSi_4O_{10}$), and Li-rich micas such as lepidolite ($K(Li,Al)_3(Al,Si,Rb)_4O_{10}(F,OH)_2$) and zinnwaldite ($KLiFeAl(AlSi_3)O_{10}(OH,F)_2$).

Tin granite-related deposits form either as syngenetic low-grade disseminated cassiterite within the hosting granites (e.g., Coetzee and Twist, 1989); as epigenetic structurally-controlled quartz-rich veins; as quartz-cassiterite (± chlorite + tourmaline) lodes (such as the classic 'Cornish lode type' deposit; Scrivener (2006)); or as greisens, i.e. intensely altered host rock where feldspars may have undergone complete breakdown (Fig. 1b). Tin deposits can be polymetallic, and sulfides such as stannite, arsenopyrite, and pyrite may be present. There is significant Cu mineralization in both the classic tin districts of southwest England and Bolivia (Jackson et al., 1989; Turneaure, 1971).

LCT pegmatites which host economic quantities of lithium are often simple and unzoned homogenous bodies consisting of subparallel megacrysts of spodumene, K-feldspar, and quartz, orientated perpendicular to the wall-rock contacts, with subordinate fine-grained albite and quartz matrix (e.g., Swanson, 2012; Sweetapple et al., 2019). Occasionally beryl, tantalite, and cassiterite are also significant components (Sweetapple et al., 2019). However, in many cases LCT pegmatites are heterogeneous zoned intrusions that record a complex multi-stage crystallization history which involves both magmatic and hydrothermal processes (e.g., Shaw et al., 2022; Stilling et al., 2006). Historically, the major crystallization / recrystallization periods invoked in pegmatites were classified by Cameron et al. (1949) as: (1) primary crystallization in concentric shells; (2) localized replacement bodies formed through recrystallization of primary features; and (3) fracture fillings along late-stage dislocations. Since this work, however, our understanding of the complex interplay of these processes in generating the various types of mineralization observed in pegmatites has developed considerably.

Magmatic crystallization in pegmatites is thought to be in part controlled by constitutional zone refinement (London, 2018). In this process, progressive crystallization from the walls inwards generates a boundary layer at the melt-crystallizing front, an interface which becomes enriched in incompatible elements and fluxing agents (e.g., F, B, H_2O). Once the boundary layer achieves the concentrations required to saturate the melt in a particular phase, this phase will then rapidly crystallize inwards as orientated megacrysts. It is envisaged that this process commonly occurs to produce spodumene or petalite once saturation is attained (>5000 ppm Li, London, 1984; Maneta et al., 2015). This, in combination with typical magmatic crystallization processes, is thought to generate the primary mineralization in a pegmatite (type 1 of Cameron et al., 1949). Upon reaching the magmatic-hydrothermal transition, several episodes of replacement can occur in a pegmatite (Kaeter et al., 2018). A common replacement mechanism is the autometasomatism of the primary magmatic mineralogy by a Na-rich magmatic fluid, a process termed albitization (Černý, 1991b; Shaw et al., 2022; Stilling et al., 2006). Albitized regions predominantly consist of fine-grained saccharoidal albite, quartz, and (lithian) muscovite (Ballouard et al., 2020; Cerny and Siivola, 1980; Shaw et al., 2022). The albitization may be massive in texture, or in other cases banded (e.g., Fuchsloch et al., 2018; Stilling et al., 2006; Wilde et al., 2021). Although minor amounts of high field-strength elements (HFSE) mineralization can occur in the magmatic stage, the predominant, and often more enriched (e.g., Kaeter et al., 2021) HFSE-bearing phases such as zircon, columbite-tantalite, and cassiterite predominantly occur during the albitization process (Ballouard et al., 2020; Morgan and London, 1987; Shaw et al., 2022; Wise and Cerny, 1990), driven by the decrease in solubility of these phases in these fluids by the progressive loss of fluxing agents Li and F (Linnen, 1998).

Post-albitization, lower temperature greisenization can occur as well, generating a quartz-muscovite (and in some cases columbite-tantalite) assemblage that replaces earlier magmatic and albitized phases (Ballouard et al., 2020; Shaw et al., 2022). Finally, low-temperature, fluid-controlled alteration can replace any of the earlier phases producing a clay-rich assemblage (Shaw et al., 2022). This low temperature alteration is commonly detrimental to the preservation of economic mineralization.

Therefore, most Li ore minerals form during the primary crystallization process, whereas Ta and Sn phases are predominantly associated with metasomatic overprints, with albitic and lepidolitic units acting as the main carriers (Černý, 1991b; Linnen, 1998). However, recrystallization of petalite to spodumene plus quartz (i.e. spodumene-quartz intergrowth or SQI) can occur during cooling. This recrystallization reflects the concept that spodumene, petalite, and eucryptite are near-polymorphs of each other, representing distinct stabilities of Li-aluminosilicates in pressure-temperature (*P-T)* space (London, 1984), and where petalite is a higher *T* phase and spodumene lower *T*.

3.5. Genetic formation models

Sn and Li deposits result from magmatic-hydrothermal systems, and largely originate from volatile-rich magmas emplaced within the mid- to upper-continental crust (Černý et al., 2005; Sillitoe, 2010). Their formation requires: silicic magma, water, metals, and volatile ligands (Cl, F, B) as essential geochemical ingredients. A genetic link between the emplacing magma and the formation of a mineral deposit is enshrined in the magmatic-hydrothermal theory of ore formation, and backed by geochemical evidence, whereby the granitic magma is viewed as the principal source of the water, metals and volatiles (Hedenquist and Lowenstein, 1994; Richards, 2011).

3.5.1. The magmatic-hydrothermal model in granites

It has long been recognized that Sn mineralization is associated with late-stage or minor intrusive bodies enriched in incompatible elements such as Sn, Li, B, Rb, and F, sometimes intruded into older unmineralized granitic bodies, and which represent a crystallization of residual melt after significant crystal fractionation (Groves, 1972). During cooling and fractional crystallization, there is a requirement to keep metals within the evolving silicate melt and further concentrate them sufficiently to form magmatic ore minerals such as cassiterite or spodumene, or to partition into hydrothermal fluids and be transported into the hydrothermal realm. The relative timing of volatile saturation versus crystallization, and the availability and partitioning of Sn and Li between melt and fluid is complex and depends on various factors including composition, temperature, and pressure (Candela, 1997; Zhao et al., 2022b).

The solubility of Sn in silicic melts strongly depends on magma composition, magma oxygen fugacity (redox), and temperature (Farges et al., 2006; Linnen, 1996; Taylor and Wall, 1992). Tin speciation – as Sn^{2+} or Sn^{4+} – has a strong influence on Sn compatibility within an

evolving magma (Ishihara, 1981; Lehmann, 1990; Ryabchikov et al., 1978); Sn^{4+} is more compatible since it has a similar ionic radius to Ti^{4+} and may substitute into minerals such as biotite. Thus, Sn typically behaves incompatibly in reducing granitic melts (Heinrich, 1990) and, in most cases, abundances increase with progressive crystallization. Cassiterite may ultimately form as a minor liquidus phase in highly fractionated portions of the system (as is seen in some pegmatites), although this requires oxidizing conditions, and is unlikely to form in reducing melts, even at the 100 ppm Sn level. Similarly, cassiterite may occur as a hydrothermal phase in highly fractionated pegmatites, possibly reflecting residual concentration and late-stage melt/fluid oxidation (Lehmann, 2021; Linnen, 1996).

In the classic magmatic-hydrothermal model (Burnham, 1979), a metal and volatile-rich melt undergoes fractional crystallization which serves to concentrate incompatible elements including Sn and Li, as well as volatile species. This concentration will attain vapour saturation (exsolution of a separate hydrothermal phase) though a combination of isobaric cooling (i.e. first boiling) and magma differentiation (i.e. second boiling). This is the magmatic-hydrothermal transition, resulting in the ponding of magmatically-derived hydrothermal fluids in the upper portions of the intrusion. According to the archetypal hydrothermal Sn model (e.g., Taylor, 1979), Sn partitions from the residual silicic melt into the fluid during exsolution, which requires the exsolving hydrothermal fluid to be capable of transporting metals (i.e. containing the ligands Cl^- and/or F^-). In granitic systems, these Sn-bearing hydrothermal fluids migrate through host rock structures, further concentrating and transporting Sn to sites where cassiterite is precipitated early in the paragenesis in lode- or vein-type deposits. These fluids are typically hot and acidic, resulting in significant alteration of the host rocks (Pollard and Taylor, 1986) variably associated with albitization, tourmalinisation, and greisenisation (Fig. 1b) during which feldspars and micas are altered to tourmaline, topaz, albite, lepidolite and quartz. Cassiterite precipitation from hydrothermal fluids may be induced either through temperature reduction, typically through a temperature range of 500–300 °C (Naumov et al., 2011) and/or by in-mixing with meteoric fluids which serve to oxidize and neutralize the acidic, reducing magmatic fluids and facilitate late-stage transformation from relatively soluble Sn^{2+} to relatively insoluble Sn^{4+} (e.g., Heinrich, 1990). Deposition of cassiterite occurs along fractures and faults to form veins and lode generations may be linked to evolving tectonic activity and stress fields (Shail et al., 2003).

Comparing the hydrothermally-dominated Sn deposits of SW England, with the pegmatite-dominated Sn deposits of Thailand, Manning (1986) suggested that varying F versus B budgets played a role, with F in particular promoting post-magmatic hydrothermal processes. Boron-rich magmas are volatile-rich and during decompression release large amounts of mechanical energy to facilitate brecciation and the formation of stockwork, whereas F-rich systems may result in more passive crystallization and disseminated cassiterite (Pollard et al., 1987).

3.5.2. Sn in pegmatite systems

Rare element pegmatites are thought to crystallize rapidly from undercooled peraluminous magmas through disequilibrium processes driven by crystal supersaturation and liquidus undercooling (London and Morgan, 2017; Sirbescu et al., 2008). Several processes are invoked to generate disequilibrium, the most prominent of which are temperature-controlled supersaturation (e.g., McCaffrey and Jowitt, 2023) or changes in vapour pressure (Simmons and Webber, 2008). Crystallization from a pegmatitic melt has been shown to be rapid (days to years), contrary to the standard belief that large crystals form slowly in igneous systems (Phelps et al., 2020; Webber et al., 1999). Rapid crystal growth in a viscous melt leads to the formation of boundary layers rich in incompatible elements and fluxes, which may serve to lower liquidus temperatures, restricting nucleation of competing mineral phases in a system and leading to the formation of abrupt layering and compositional changes within a pegmatitic body (London, 2008). This process is invoked to produce the various crystallization textures observed within pegmatites (Černý, 1991b; Norton, 1983). The boundary layer produced at the interface of the crystallizing front and the remaining melt can lead to localized enrichment of Sn, driving magmatic precipitation of cassiterite (Kaeter et al., 2021; London, 2014). Magmatic cassiterite, however, typically only occurs as an accessory phase in pegmatites (Hulsbosch and Muchez, 2020; Kaeter et al., 2018; Suwimonprecha et al., 1995). As mentioned, the majority of cassiterite mineralization in pegmatites occurs through hydrothermal processes. Upon reaching the magmatic-hydrothermal transition, in situ metasomatism commonly occurs, replacing the primary magmatic mineralogy through albitization and greisenization (Shaw et al., 2022). The residual hydrothermal fluid in a pegmatite commonly carries complexing ligands (e.g., F and B) capable of keeping Sn mobile in aqueous solution (Kaeter et al., 2021; Wood, 2005). The fluid-rock reactions driving the albitization process (e.g., by replacing K-feldspar with albite + muscovite, or decreasing salinity) in pegmatites changes the chemistry of the fluid which can promote the precipitation of oxides (Ballouard et al., 2020; Hulsbosch and Muchez, 2020).

3.5.3. Li in granite-pegmatite systems

Progressive magma fractionation during crystallization drives the enrichment of Li in the residual melt. Until saturation of Li minerals is achieved, Li will remain in the residual system and can therefore be carried into the hydrothermal fluids (London, 1986). In this way, late-stage alteration of primary magmatic micas to form lithium-rich varieties (e.g., lepidolite and zinnwaldite) is commonly associated with the albitization process (Breiter et al., 2023a, 2023b; Guimarães et al., 2021; Legros et al., 2016; Monnier et al., 2022; Putzolu et al., 2024). Granitic lithium deposits are therefore predominantly hydrothermal in origin. In contrast, since Li-rich pegmatitic melts have initial Li contents orders of magnitude above typical granitic levels (Stilling et al., 2006), Li mineral saturation is more frequently achieved in the magmatic state in pegmatite systems (Maneta et al., 2015). Pegmatite Li-ore deposits (consisting of the silicates spodumene and petalite) are therefore magmatic in origin, with later-stage metasomatic processes being detrimental to the preservation of Li mineralization.

Sufficiently concentrating incompatible elements such as Sn or Li to generate economic deposits is dependent on either extreme degrees of crystal fractionation, or alternatively extracting low-degree partial melts away from a melting source rock. These two processes form the basis of the dominant pegmatite petrogenetic models: (i) extreme fractionation of granitic melts that carry average incompatible element abundances, producing a volumetrically minor volatile-rich melt that migrates from the parent body to generate pegmatites (Cameron et al., 1949; Černý, 1991a; Černý et al., 2005; Jahns, 1953); or (ii) small melt extractions of low-degree partial melting of metal–rich host rocks during metamorphism, similarly generating a volatile-rich melt (Müller et al., 2017; Shaw et al., 2016; Simmons et al., 1995; Stewart, 1978). Alternative models consisting of some combination of these processes have been proposed, because single-stage enrichment processes alone are likely inadequate to achieve the required Li concentrations to saturate Li ore minerals (Koopmans et al., 2023).

4. Crustal evolution toolkit

Mineral deposits are the products of ordinary geological processes, many of which also drive the growth, evolution, and differentiation of Earth's continental crust (e.g., Cawood and Hawkesworth, 2015). These processes exert a fundamental control on the propensity of granites to be metal-fertile (e.g., Černý et al., 2005). Over the last two decades there has been a revolution in our understanding of crustal genesis and evolution, through the application of mineral-based petrological and geochronological tools and the development of new thermodynamic melt models used to simulate melting processes within the lithosphere. In doing so, we can take both an inverse (empirical) and forward

modelling (predictive) approach to the problems of crustal melting and differentiation. Here we discuss these fundamental tools.

4.1. Mineral-based petrological tools

The widespread availability of laser ablation-inductively coupled mass spectrometry (LA-ICPMS), which can analyze in situ trace elements and isotopes in a range of mineral archives, has driven a revolution in our understanding of crustal evolution. Such techniques have been specifically applied to minerals that are physically durable and chemically stable over a wide range of physico-chemical conditions encountered within the crust and at the Earth's surface. These individual minerals are less susceptible than whole-rock chemistry to subsequent geological events that may involve the loss of fluid-mobile elements and/or disturbance of isotopic systems.

The principal mineral of choice for this approach has been zircon (Belousova et al., 2002a; Kemp and Hawkesworth, 2013), which is common in evolved magmatic rocks and is chemically robust, allowing it to survive a range of geological processes that can impinge upon the reliability of whole-rock data (Roberts and Spencer, 2015). Zircon saturation occurs relatively early during granite evolution, which makes it a reliable monitor of the evolution of its parental magmas (Hoskin, 2003; Kemp and Hawkesworth, 2014; Valley, 2003). Further, zircon has a high closure temperature, can be precisely dated via U—Pb isotopes, hosts a range of other useful isotopic tracers (e.g., Hf, O, Si) and trace elements and metals, and has relatively low diffusivities for certain species, ensuring that chemical fidelity is maintained with respect to chemical zonation (Cherniak, 2010). Inherited (typically cores) and xenocrystic zircons are common in granites, yielding information regarding earlier melting cycles.

There has been increased interest in the application of these tools to metallogenic problems – albeit with distinct challenges. Such studies have investigated the use of zircon chemistry as well as other accessory and major mineral phases such as apatite, titanite (in conjunction with zircon), as well as mica and feldspar, both to better understand mineralized systems, and as so-called pathfinders to prospective areas of granite-hosted mineralization. These studies initially focused on Cu-Au (—Mo) porphyry deposits (Ballard et al., 2002; Belousova et al., 2002b; Dilles et al., 2015; Lu et al., 2016; Mao et al., 2016; Williamson et al., 2016).

One of the major difficulties in applying the above granite-focused mineral tools to LCT pegmatite systems is the scarcity of common geochronometers such as zircon (Stilling et al., 2006). Where such phases are present, they are often highly metamict (Lupulescu et al., 2011) making robust geochronology challenging in phases that are commonly considered refractory. Further, the extensive volatile content of such systems can serve to significantly overprint mineral chemistry, or even replace minerals in their entirety. The abundance of the low-temperature alteration within both granitic and pegmatitic systems that is important for mineralization has driven the development of new geochronological techniques to track magmatic-hydrothermal processes in Sn—Li systems, using non-standard phases such as columbite-tantalite, cassiterite and lithian muscovite. These have been applied to pegmatitic systems, as discussed below.

4.1.1. Geochronology

Understanding the timing and timescales of mineralization and of related granites is important for building 4D metallogenic models during long-lived geodynamics, and linking mineralization events to magmatic phases. Zircon U—Pb is a key chronometer for granite dating given its ubiquity, compatibility of U, and its high closure temperature (Scherer et al., 2007). However, constraining the age of pegmatites can be quite challenging. As mentioned, zircon is often absent in pegmatites, or if present, is often highly metamict due to the typically high concentrations of U. High U concentrations lead to progressive destruction of the zircon crystal structure due to damage from U breakdown, resulting in the loss of interstitial Pb and disturbing the U—Pb isotope systematics. Thus, alternative approaches have been taken to dating pegmatite magmatism, including: Pb—Pb on apatite; U—Pb on apatite, xenotime, monazite, allanite, tantalite; Re—Os on molybdenite; and Ar—Ar on mica (Bradley et al., 2016; Camacho et al., 2012; Hetherington et al., 2021; Kontak et al., 2005; Popov, 2023; Shaw et al., 2016). Given the variable precision of many of these approaches, and the nature of dating volatile-rich bodies, workers sometimes apply several methods to constrain the crystallization age of a pegmatite. In a study of the Tanco LCT pegmatite, Manitoba, Camacho et al. (2012) applied a variety of different radiogenic isotope approaches to constrain the age of the intrusion, including tantalite U—Pb (2641 Ma); zircon U—Pb (2660–2606 Ma); Pb—Pb isochron on mica and feldspar (2657 Ma); and lepidolite Rb—Sr (2631 Ma). However, pegmatite geochronology remains a challenging endeavour, and novel chronometers are now coming onstream, such as Rb—Sr on minerals such as micas and apatite, and Lu—Hf on garnet (Glorie et al., 2024; Zack and Hogmalm, 2016).

Whilst zircon and other silicate mineral chronometers can help provide an age for a hosting granite or pegmatite to varying degrees of effectiveness, the ability to date mineralization events is of particular importance to interrogate pulsed, sporadic mineralization during long-lived, protracted magmatism, or to yield a magmatic age for a pegmatite body where the magmatism and mineralization are assumed coeval. Early efforts to date Sn mineralization used geochronology of assumed coeval minerals. An example is the combination of Rb—Sr dating of quartz inclusions, Re—Os dating of molybdenite, and Th-U-Pb dating of uraninite applied to tin-bearing granites of the Erzgebirge region which allowed Romer et al. (2007) to constrain the ages of primary tin mineralization to a narrow range of 318–323 Ma.

A alternative approach that is still being developed is the use of dating of ore minerals to directly measure the age and timing of mineralization events within long-lived magmatic systems. Columbite-tantalite group minerals (CGMs, i.e. Ta—Nb oxides) have shown remarkable potential in pegmatite systems for constraining Ta mineralization and by inference the age of the pegmatite (Romer and Lehmann, 1995; Romer and Smeds, 1996). CGMs are capable of accommodating U whilst excluding Pb almost completely during crystallization, hence can develop high radiogenic Pb compositions over geological timescales (Melcher et al., 2015; Romer and Wright, 1992). Recently, sufficiently robust reference materials have been characterized, and standard protocols for in situ U—Pb analysis of CGMs by both LA-ICPMS and SIMS has been established (Che et al., 2015; e.g., Legros et al., 2019; Smith et al., 2004). Linking U—Pb with other isotopic and geochemical data from CGMs has been shown to provide insights into the source and internal evolution of pegmatites prior to Ta mineralization (Kendall-Langley et al., 2020; Melcher et al., 2015).

Perhaps the most promising new chronometer for Sn—Li systems is cassiterite U—Pb. Cassiterite can contain up to 100 ppm U and variable-low amounts of common Pb, making it a prospective geochronometer. Dating cassiterite has the potential to constrain the timing of Sn mineralization and also associated co-genetic Li, W etc. mineralization. Cassiterite is a robust mineral, so digestion is challenging, however high precision ages can often be yielded via isotope dilution thermal ionization mass spectrometry (ID-TIMS) giving superior constraints on the timing of tin mineralization during long-lived magmatic systems (Goodey et al., 2023; Tapster and Bright, 2020). Since the earliest attempts to apply cassiterite geochronology using ID-TIMS (Gulson and Jones, 1992), the technique has been refined to yield precisions as high as <0.1 % (Tapster and Bright, 2020). At the same time, the rapid development of in situ techniques has meant that U—Pb analysis of cassiterite via both SIMS and LA-ICPMS is becoming more widespread (Carr et al., 2017).

Combining geochronometers and trace element data offers unique opportunities to reconstruct the timing of magmatic-hydrothermal processes. For example, Cheng et al. (2019) used cassiterite trace elements to understand controls on hydrothermal cassiterite deposition,

and coupled this with cassiterite U—Pb geochronology to understand the development of the hydrothermal system; Kendall-Langley et al. (2020) used a combined cassiterite and columbite-tantalite U—Pb approach to constrain the age of Sn—Ta pegmatite mineralization in the Pilbara Craton.

4.2. Modelling partial melting and melt metal endowment

Generation of Sn and Li-bearing granitic magmas is the end result of high-grade metamorphism leading to crustal anatexis. The *P–T* conditions needed to drive partial melting are commonly reached during tectonism in collisional orogenic settings (Copley and Weller, 2022). Andean-type magmatism above subduction zones may also locally elevate ambient crustal geotherms in a continental arc, although do not typically lead to widespread partial melting of the arc crust itself (Cawood et al., 2009), accounting for the observation that pre-collisional S-type granites are absent from such environments. Most magmatism that occurs in accretionary orogens is driven by melting of the underlying asthenospheric mantle wedge, situated above a devolatilizing subducted slab (Hawkesworth et al., 1993; Poli and Schmidt, 2002). While such arc magmas may undergo fractional crystallization during ascent or assimilate small volumes of country rock in order to achieve a granitic (sensu lato) bulk composition, these intrusions remain infertile with respect to Sn—Li mineralization.

Partial melting of continental crust occurs primarily through the breakdown of hydrous minerals such as mica and amphibole, and can be either thermally driven (i.e. dehydration melting) or facilitated through the ingress of fluids, which serve to lower the solidus (i.e. water-present melting). The *P-T* conditions at which key melting reactions take place, and the approximate volume of melt produced by each, may be constrained by experimental petrology (Fig. 3). The data derived from such procedures allow development of conventional thermobarometers for use in determining the *P* and *T* conditions reached by natural granites and their host rocks (e.g., Anderson, 1996), alongside thermodynamic models that can be used to predict the mineral-fluid-melt assemblages that stabilize in a given protolith in a range of geological scenarios, including regional and contact metamorphism (e.g., Powell and Holland, 2008). This latter technique – broadly referred to as phase equilibrium modelling (PEM) – has since the late 2000s revolutionized the field of quantitative petrology, and is being continuously developed as advances are made in software development, and thermodynamic datasets and models are expanded to incorporate elements relevant to ore genesis (Kelsey and Powell, 2011).

In metasedimentary rocks, Sn is primarily hosted in muscovite, biotite, titanite and rutile, whereas Li is mainly held within biotite, muscovite, cordierite and staurolite (Kunz et al., 2022; e.g., Simons et al., 2017). Breakdown of these phases serves to enrich a melt in Sn and Li. Early attempts to broadly link melt source rock to granite type were made by Strong (1981), who built a framework from the various melt products of muscovite, biotite and amphibole-rich protoliths. In his model, water-rich crustal melts formed through the anatexis of micaceous rocks, such as schists, which themselves resulted from metamorphism of clay-rich material (e.g., mudstones). Subsequent experimental work (Patiño-Douce and Johnston, 1991; Vielzeuf and Holloway, 1988), which has since been backed up by PEM investigation (White et al., 2007), has shown that muscovite and biotite decomposition are the main drivers for the production of large volumes of granitic melt in orogenic systems. Nonetheless, while mudstones represent extremely fertile source rocks, they typically comprise minor proportions of continental sedimentary successions. Instead, greywackes dominate, yet they contain a lower initial clay content, making them relatively less fertile (Montel and Vielzeuf, 1997). Melting driven by amphibole breakdown is restricted almost exclusively to meta-igneous and/or meta-volcanic rocks, such as basalt, which first undergo wet melting at upper amphibolite-facies conditions (Palin et al., 2016). Nonetheless, while amphibole breakdown can produce large volumes (>30–40 %) of melt at mid/lower crustal conditions, these fractions are K-poor and have compositions of trondhjemite, tonalite, or granodiorite composition – not granite (Helz, 1976; Moyen and Martin, 2012).

The major element composition of a partial melt is largely controlled by the mineral breakdown reactions that take place. For example, mica dehydration melting yields an Al- and K-rich melt, whereas amphibole breakdown produces a melt which is more sodic (Moyen, 2020). Melt trace element concentrations, however, are controlled by both the mineral breakdown reactions that take place, and the partitioning of that trace element between the melt and restitic minerals – i.e. their compatibility. Determining the stability of rock-forming minerals and the partitioning of trace elements between residual phases and an evolving melt requires simultaneously assessing the importance and role of a wide range of petrological variables (e.g. *P*, *T*, a_{H2O} etc.). As such, conventional forward (predictive) models of metal-bearing granite generation via modal/closed-system melting during metamorphism

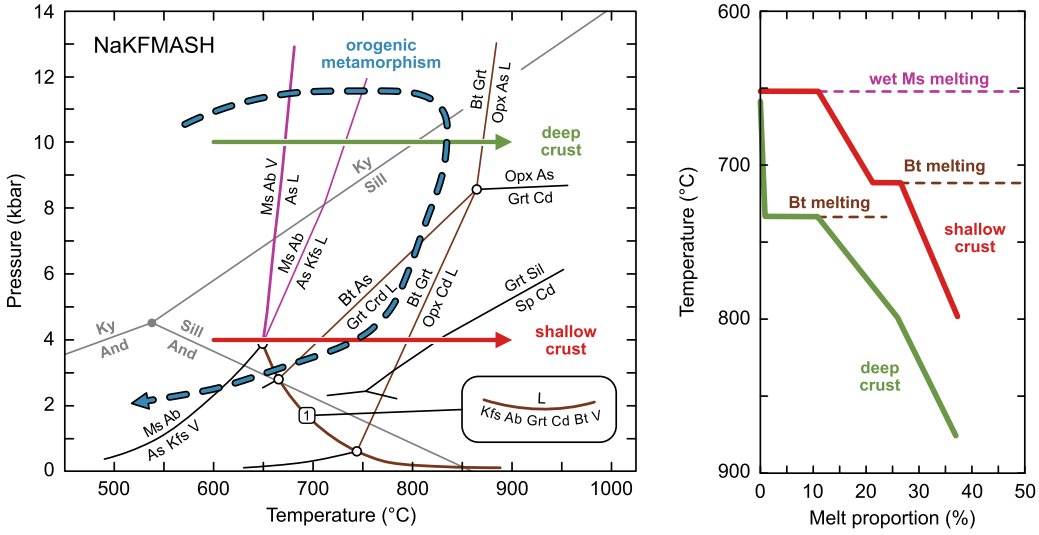


Fig. 3. Pressure-temperature (*P-T*) diagram showing key melting and dehydration reactions in the Na_2O-K_2O-FeO-MgO-Al_2O_3-SiO_2-H_2O (NaKFMASH) system (left) and volumes of partial melt production during isobaric heating in the upper and lower crust (right) (Spear et al., 1999). Blue *P-T* path represents an example burial and heating path during followed during collisional orogenesis (Imayama et al., 2019). (For interpretation of the references to colour in this figure legend, the reader is referred to the web version of this article.)

have been superseded by more complex thermodynamic models that allow investigation of non-modal/open-system melting processes, which in turn assesses the evolution of restitic phases during melt production and continuous metamorphism. Complementary software tools developed by the igneous petrology community (e.g., MELTS; Guaida et al., 2012) may be used to examine the cooling and crystallization history of melt fractions as they ascend through the crust, including considering interactions with wall rocks (Heinonen et al., 2020).

5. Crustal Evolution and Sn—Li Metallogeny

The key processes and conditions in the development of Sn—Li bearing magmatic-hydrothermal mineral deposits that can be monitored using a crustal evolution toolkit are (Fig. 4):

i. Source and conditions of melting - i.e. the composition of the crustal source; how melting is induced; degree of melt and conditions of melt, e.g. *T, P,* a_{H2O} all impose a geochemical inheritance on the melt;
ii. Fractional crystallization and melt evolution – this drives metal concentration and volatile saturation;
iii. The availability of volatile ligands in the vapour phase, and of other volatiles;
iv. The availability of metals in the melt, which depends on redox state and the degree of fractionation;
v. Metal mobility and partitioning between source, melt, and hydrothermal fluids during magma degassing;
vi. Geodynamics, regional geology, and crustal architecture which impose controls on source and the conditions of melting.

Here, we review the various approaches taken to understand these processes and conditions, using case studies where relevant.

5.1. Magmatic source

Although much metallogenic research has focused on the processes that occur during the ascent and cooling of granitic melts, on the behaviour of exsolving hydrothermal fluids, and on the partitioning of elements between the phases present (Candela, 1992; Whitney and Naldrett, 1989), the fundamental question of how a granite magma originally became endowed with the metals of interest has rarely been addressed. In order for these various ore-forming mechanisms to operate and concentrate metals, those metals must occur in the melt in the first place, and this is primarily controlled by (a) the magmatic source, and (b) by the melting process. Magmatic source, namely the inherited properties of the lithospheric domain from which a granitic melt is extracted, imposes a geochemical heredity onto the evolving magma system and also determines the initial metal and volatile contents of the magmas (Blevin and Chappell, 1995; Hart et al., 2004).

5.1.1. Constraining source characteristics via accessory mineral chemistry

Mineral chemistry can be used to monitor magmatic processes, and the use of zircon has historically been a common choice. Breiter et al. (2016) analyzed a range of trace elements in zircons taken from the different granite suites that comprise the Cornubian batholith. They used the zircon Zr/Hf ratio as a monitor of magmatic fractionation (Linnen and Keppler, 2002), and through this linked the less evolved biotite granite suite to the more evolved topaz suite. Zircon rare earth element anomalies have been proposed as useful oxy-barometers – specifically the cerium (Ce) anomaly (Ce/Ce*; Ballard et al., 2002; Trail et al., 2024), since unlike most rare earth elements (REEs), Ce can exist in two valence states: 3^+ and 4^+. Similarly, the europium (Eu) anomaly (Eu/Eu*) has been proposed both as a measure of oxidation state, and of magma fractionation, the latter as it monitors plagioclase crystallization (Gardiner et al., 2017; Roberts et al., 2024; Yakymchuk et al., 2023).

Using these tools, Gardiner et al. (2017) explored replicating the classic study by Blevin and Chappell (1992) of the mineralized granites of the Lachlan Fold Belt (LFB) of southeast Australia, through the lens of zircon chemistry. In the original study, whole-rock granite chemistry was linked to metal deposit affinity using Rb/Sr and Fe_2O_3/FeO as fractionation and oxidation proxies respectively. Blevin and Chappell (1992) highlighted that less fractionated, more oxidizing (i.e. lower Rb/Sr; higher Fe_2O_3/FeO) I-type monzogranites are typically associated with porphyry Cu-Au-Mo deposits, whereas those that contain significant Sn—W mineralization tend to be more fractionated, reducing S-type granites. Gardiner et al. (2017) analyzed zircons taken from representative samples from the paired Cu—Au and Sn—W granite belts found in Myanmar. These coeval I- and S-type magmatic belts respectively formed within an accretionary margin (Gardiner et al., 2015a). Fig. 5A shows average zircon Eu/Eu* versus Ce/Ce* compositions (respectively proxies for fractionation and oxidation state) for the Myanmar belts. A striking association was observed between granites with high whole-

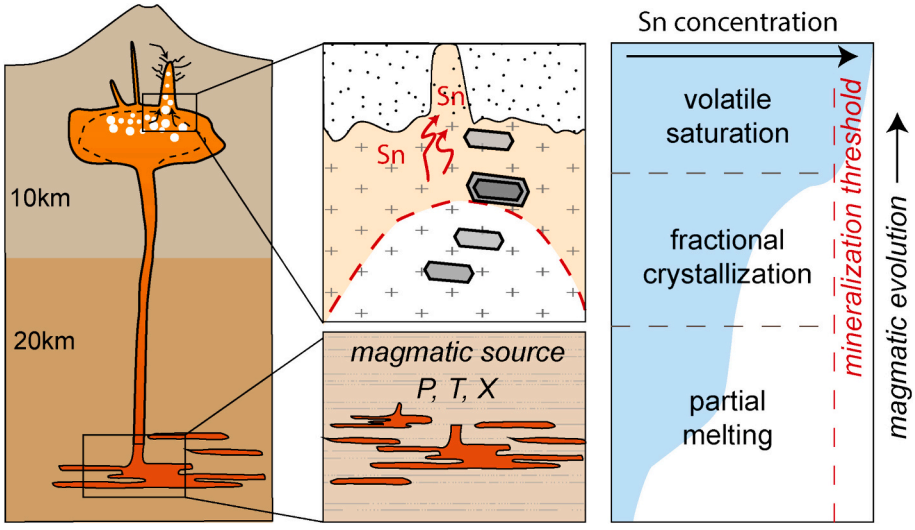


Fig. 4. A schematic of the processes involved in the development of Sn, and by extension Li, mineralization: (i) partial melting of a source; (ii) the ascent and emplacement of the melt and accompanying fractional crystallization; and (iii) vapour saturation which may partition metals into the exsolved hydrothermal fluid. Also shown schematically is (centre) how these processes may be monitored using melt modelling and mineral chemistry, and (right) how Sn may be concentrated during these processes leading to eventual mineralization via saturation of ore minerals above a given threshold.

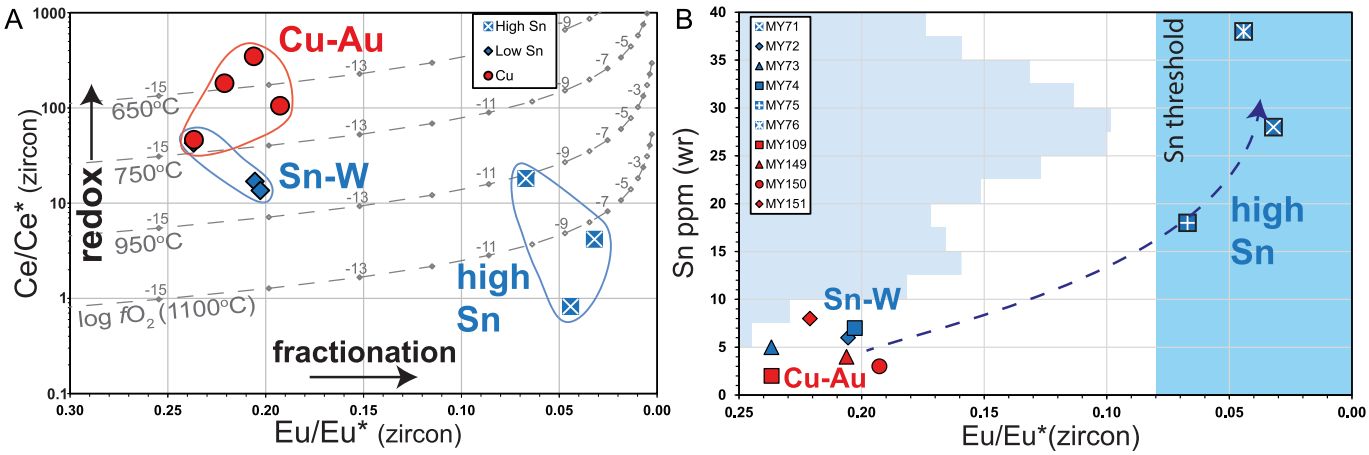


Fig. 5. A: Plot showing zircon Ce/Ce* (i.e. oxidation proxy) and Eu/Eu* (fractionation) from the Myanmar paired Cu—Au and Sn—W magmatic belts. Cu-hosting granites are oxidizing and less fractionated; Sn-rich granites are reducing and more fractionated. Dotted lines reflect modelled isothermal co-variance of Ce/Ce* and Eu/Eu* as a function of fO_2. B: Plot of whole-rock Sn content against average zircon Eu/Eu* for the same samples. Blue box represents a 'threshold' level of Sn, suggesting a zircon Eu/Eu* of 0.08 or less may indicate elevated Sn values and the potential for the development of Sn mineralization. Also plotted on the y-axis are aggregated and bucketed whole-rock Sn contents reported for major tin deposits from Southeast Asia (Malaysia and Thailand), the Erzgebirge, Bolivia, Portugal, Nigeria, and the Massif Central, as summarized in Lehmann (1990). Both plots from Gardiner et al. (2017). (For interpretation of the references to colour in this figure legend, the reader is referred to the web version of this article.)

rock Sn contents and those with pronounced zircon Eu/Eu* (Fig. 5B), a link which allowed the authors to explore an Eu/Eu* 'threshold' associated with the high Sn granites (see section on fractionation). Similarly, Li et al. (2019) also looked at coupled zircon Ce and Eu anomalies to distinguish between Cu—Mo and Sn-related mineralization.

These examples highlight the potential of zircon trace elements as monitors of metallogenesis. However, the issues concerning zircon in some granites and pegmatites has focused attention on other accessory mineral chemistry. For example, Sha and Chappell (1999) suggested that apatite from S-type granites shows higher Mn and Fe, lower light REE and Th, and stronger negative Eu anomalies than apatite from less evolved and more oxidized I-type granites. A study on apatite chemistry across the compositional spectrum from carbonatites and lherzolites to granites and pegmatites found that Sr, Y, Mn, Ce/Yb_N and Eu/Eu* signatures can distinguish broadly different igneous environments (Belousova et al., 2002b). Ding et al. (2015) showed that the trace element and Sr isotope composition of apatite may reflect the nature of source rocks and associated mineralization: granodiorite porphyries hosting Cu-Pb-Zn mineralization have significant mantle input and are oxidized, whereas granites with Sn—W granites show limited input of mantle material. These examples suggest that accessory mineral chemistry is a powerful tool to constrain granite source and metallogenic affinity.

5.1.2. *Isotopic constraints on magmatic source*

Geochemical evidence has long supported the concept that Sn and Li bearing granitic melts are typically formed from partial melting of pre-existing continental crust. Their peraluminous nature (i.e. Al- and K-rich), the presence of significant B contents and the common association of tourmaline implies Sn and Li granites and pegmatites are highly evolved melts derived from partial melting of a clay-rich metasedimentary protoliths (London and Morgan, 1996; Strong, 1981). Such sedimentary material is highly melt-fertile via muscovite and biotite dehydration melting, and is often found in association with major Sn deposits such as the Bolivian tin belt of the Eastern Cordillera and the Cornubian batholith (Coward, 1990; McBride et al., 1983).

Isotopes are key tools for tracing partial melting events and the various crustal reservoirs involved. Long-lived radiogenic isotopes systems such as ^{147}Sm—^{143}Nd, Rb—Sr, and Lu—Hf can trace the evolution of these reservoirs to yield timescales since melting (i.e. crustal residence time) and were traditionally applied to granites at the whole-rock level. Such studies on Sn-bearing granites revealed signatures indicating dominantly or mixed crustal-derived sources (Cobbing et al., 1986; Lehmann, 1990) with in some cases evidence of mantle input (Darbyshire and Shepherd, 1994; Walshe et al., 2011).

Stable isotope systems are also useful in tracing melt sources, and systems such as O are sensitive to low-T (<~200 °C) surface processes such as weathering and hydrothermal alteration, and thus can monitor the incorporation of sedimentary material into the melt. Ashworth et al. (2020) studied feldspar and quartz O isotopes in the Namibian pegmatite belts, highlighting differences between U-bearing NYF pegmatites and leucogranites ($\delta^{18}O$ = 11–13 ‰) and Sn-Li-Ta bearing LCT-types ($\delta^{18}O$ = 14–16 ‰). They inferred the U-bearing pegmatites as representing a mixed metasedimentary and igneous source, and the Sn-Li-Ta pegmatites to be pure metasedimentary melts. Romer et al. (2014) explored the novel isotope systems of B and Li to compare the Variscan granite suites of the Erzgebirge region with potential protoliths. Their results were however equivocal, showing that there was limited range in $\delta^{11}B$ and $\delta^{7}Li$ that might otherwise provide more information on source characteristics.

Combining radiogenic and stable isotope studies yields additional information to constrain melt source, and perhaps the most powerful such isotopic tracers in granites are coupled zircon Hf and O isotopes (Kemp et al., 2007). An example of how combined zircon Hf—O isotopes can be applied to Sn metallogeny is that of the granite belts of Southeast Asia, which comprise four principal belts: (i) Sn—Li bearing Late Cretaceous-Eocene Western Province in Myanmar and Thailand (Chhibber, 1934; Gardiner et al., 2018; Khin Zaw, 1990) – i.e. the "Myanmar tin belt"; (ii) Sn-bearing Triassic S-type Main Range Province; (iii) Permo-Triassic I-type Eastern Province representing pre-collisional arc-type magmatism; and (iv) Eocene–Miocene Cu—Au bearing magmatic arc in western Myanmar (Cobbing et al., 1986; Hutchison, 1977; Searle et al., 2012). Gardiner et al. (2018) analyzed zircon Hf—O isotopes from the four belts (Fig. 6A) and showed that the mantle-like $\delta^{18}O$ (5.3 ‰; Valley (2003)) and radiogenic Hf isotopes measured in the Cu arc rocks imply that these were juvenile melts extracted from the mantle with limited crustal component. In contrast, the three tin granite belts record unradiogenic Hf isotope values implying they were in part derived from the melting of much older (up to 1.5 Gyr) crustal material. In particular the Myanmar tin belt clearly exhibits heavy zircon $\delta^{18}O$ up to 8 ‰ (Fig. 6B), suggesting that these Sn-bearing granites formed from melting older crustal material that experienced low-temperature surface

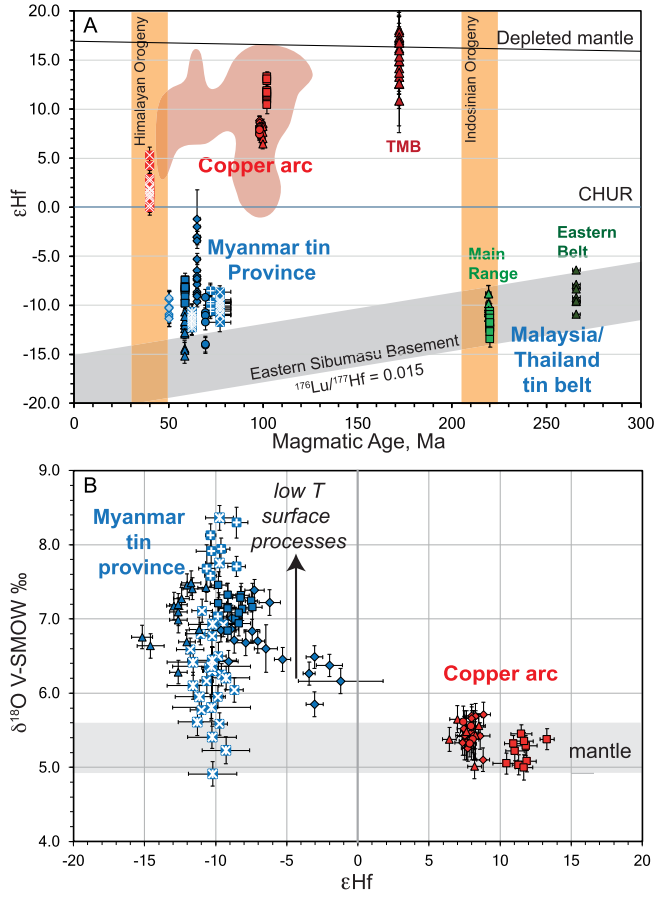


Fig. 6. A: Hf evolution diagram plotting zircon magmatic age versus zircon Hf isotope data from the major granite belts in Myanmar. B: Plot of zircon εHf versus $\delta^{18}O$ for samples from the tin belt and the copper-hosting magmatic arc. After Gardiner et al. (2018).

weathering processes.

Radiogenic isotopes such as Hf, Nd and Sr, also have potential for constraining the origin of LCT pegmatites, and workers have compared the isotopic signatures of pegmatites with surrounding country rocks to trace the source of the melts. Whilst Hf isotope systematics in cassiterite are still poorly understood, a reconnaissance cassiterite Hf isotope study of LCT pegmatites in the Pilbara Craton showed promise for linking the pegmatites to potential parental rocks (Kendall-Langley et al., 2020). There is also potential for Nd isotopes in accessory minerals to provide a genetic link to source. By example, Tomascak et al. (1998) analyzed monazite and apatite Nd isotopes in two groups of pegmatites in Maine and in spatially associated granites and metasedimentary-derived migmatites. Whilst not LCT-type pegmatites, the authors showed that (a) the two pegmatite swarms have different initial Nd isotope values, forming coherent groups, and (b) that each swarm can be isotopically linked to different putative sources, be it granites or country rock.

5.1.3. *Source pre-enrichment*

The formation of economic Sn—Li deposits requires that melts become enriched in metals significantly above ordinary crustal abundances. In particular, crystallization of Li ore minerals such as spodumene and petalite requires Li melt concentrations in excess of 5000 ppm (London, 1984; Maneta et al., 2015) – approximately 250 times higher than mid-crustal values (Rudnick and Gao, 2014). Furthermore, to form economic-grade LCT pegmatites, concentration must occur relatively early in the crystallization history to enable early saturation of Li-bearing minerals.

This highlights a fundamental question: do the processes of partial melting and fractional crystallization sufficiently concentrate economic metals to the point where they behave like a major element, or does the magmatic source need elevated contents of these metals (i.e. pre-enrichment)? This latter case would point to a particular set of prior geological processes to deliver metal-rich sedimentary material down to the melt zone to ultimately form metal-rich melts.

Accordingly, some workers, notably Romer and Kroner (2016), argue strongly for metal source enrichment as a necessary prerequisite to the formation of both Sn granites and LCT pegmatites. Protolith Sn and Li contents principally control metal concentrations for a given melt fraction. Thus, protolith metal pre-enrichment decouples the requirement for melting processes alone to deliver sufficient melt concentrations of metals, i.e. through the anatexis of metal-rich sedimentary material. Intense chemical weathering of continental crust produces sedimentary material depleted in elements associated with feldspars - e.g., Sr, K, Ca, Eu - but enriched in those elements preferentially concentrated in clays such as Rb, Cs, Sn, W, B and Li (Romer and Kroner, 2015; Teng et al., 2010). These clay-rich sediments may then be buried to form part of the protolith, and which will during early (low-grade) metamorphism transform into metapelitic material. However, estimates of 'average' metapelite Sn and Li concentrations vary, and initial contents are subject to later modification as Li especially is highly mobile during hydrothermal alteration and can strongly diffuse through crustal rocks (Linnen et al., 2012). To assess 'reasonable' upper bounds for average Sn and Li contents in melt-fertile clay-rich sediments, Koopmans et al. (2023) compiled published data from sediments globally and yielded ~4 ppm Sn and ~ 120 ppm Li. These baselines suggest that minimum concentration factors of some 10× (Sn) and 50× (Li) respectively would be required during partial melting and crystallization to yield Sn and Li ore minerals, highlighting especially in the case of Li the extreme enrichment required of these processes to form primary petalite/spodumene. Melting a protolith with initial Sn and Li concentrations significantly elevated over these values would potentially permit ordinary melting and crystallization processes to result in mineralization, in this case implying that the primary control on whether granites are mineralized or not is the degree of protolith enrichment. Li in particular has been found enriched in evaporitic sediments (Roda Robles et al., 1999) and in Li-rich clay minerals such as hectorite (Starkey, 1982).

An alternate view, proposed by Lehmann (1982), is that protolith metal enrichment is subordinate to differentiation processes - at least for Sn. Lehmann suggested there is little or no evidence for anomalous Sn enrichment in the likely source rocks adjacent to the major tin granite belts, concluding that Sn enrichment in granites associated with primary deposits is the result of pronounced in situ crystal fractionation and partitioning of incompatible trace elements into an exsolved aqueous magmatic-hydrothermal phase. However, if fractionation alone were all that is required to reach the point of metal saturation, then mineralized granites should arguably be more common. This is especially pertinent since Sn granites and economic LCT pegmatites tend to form in a small number of specific metallogenic provinces, whilst the widespread occurrences of barren granites and pegmatites – which are thought to have formed in similar tectonic settings – gives strength to a simple explanation of geochemical hereditary (Schuiling, 1967). Moreover, a survey of published trace element data for apatite associated with Sn mineralization (Mangler et al., 2024) shows that barren and mineralized granites are often similarly fractionated and reduced (as constrained by strongly negative Eu/Eu*, high Mn, low Sr/Y), indicating similar petrogenetic histories. By contrast, apatite Li and Sn concentrations appear to be consistently elevated in mineralized rocks relative to barren intrusions (see Section 5.3.3).

5.2. *Partial melting and melt metal endowment*

An alternative approach to constrain the role of source enrichment is to model the melting process and determine enrichment factors during partial melting. Several recent studies have used equilibrium

thermodynamic-based phase equilibria modelling tools to investigate how melt is endowed by metals during crustal anatexis, and so identify the major controlling factors.

Wolf et al. (2018) performed forward modelling to examine the contrasting melting behaviour of deeply weathered and altered versus unaltered shale in a regional metamorphic environment representative of collisional orogenesis. They explored how protolith composition and melting conditions affected trace element partitioning between melts and restites for low-temperature and high-temperature migmatites. They showed that Sn is primarily hosted in muscovite, biotite, titanite and rutile, and thus the stability and/or breakdown of (especially) mica significantly controls melt Sn endowment. A key outcome from this study was that the removal (extraction) of melts generated at relatively low temperatures, for example via muscovite breakdown, will serve to retain and enrich Sn in the restitic biotite. This means that subsequent melts generated at higher temperatures following biotite decomposition will be somewhat more enriched in Sn than if the melt is generated and retained in the source region throughout the entire metamorphic/magmatic cycle. Furthermore, metal enrichment during partial melting was noted to be particularly more efficient in pelitic protoliths that had experienced intense chemical alteration before burial, as per Romer and Kroner (2016). Such weathering causes leaching of highly mobile elements, such as Na and Ca, resulting in relative enrichment of K and favouring the stabilization of mica-rich metamorphic mineral assemblages at depth in the crust.

This work was built upon by Zhao et al. (2022a) who investigated the melting reactions that formed distinct W- and Sn-bearing granitic intrusions in various deposits worldwide. They showed that W-rich granites typically formed from muscovite-breakdown melt-producing reactions at relatively low temperatures (cf. Fig. 3), whereas Sn-rich granites typically formed from biotite-breakdown reactions at higher temperatures. These natural data were supported by modelling results showing that the most important donors of W and Sn to partial melts formed in metapelitic systems are muscovite and biotite, respectively. As such, shallow melting during orogenic burial of pelitic sediments should generate W-rich magmas that are younger than deeper-sourced Sn-rich magmas generated later during the orogenic cycle at greater crustal depths.

Kunz et al. (2022) advanced on the work of Zhao et al. (2022a) by studying the metal contents of natural micas from Barrovian-type (regionally metamorphosed) metapelites from the Central Himalayas. At the highest metamorphic grade, these had begun to partially melt, allowing examination of partition coefficients for certain metals between mica and melt as a function of *P-T* conditions. Their data showed that biotite contained relatively higher concentrations of Li, V, Co, Cs, and Ta concentrations, whereas muscovite contained relatively higher In, Sn, and W contents in any given sample that contained both micas. With progressive anatexis at higher temperatures, both micas demonstrated progressive depletion in Sn contents, indicating that Sn had been concentrated into the coexisting granitic melt. Given the propensity for muscovite to be consumed at relatively lower temperatures than biotite, Kunz et al. (2022) also indicate that granulite-facies melts forming in the deep crust are likely to have acquired all of their Sn solely from biotite breakdown.

Whilst extremely small degrees of melting (e.g. <5 %) leads to melt enrichment in incompatible elements, in practice it is considered difficult to extract such low-volume melts from their source. In the earliest stages of anatexis, melt droplets form along intersections between reactant minerals that may be widely distributed within a rock. As a result, incipient melt occurs in isolated domains that remain trapped at depth within the crust. Experimental petrology has shown that interconnectivity of melt along grain boundaries occurs once its volume reaches ~7 % (Rosenberg and Handy, 2005), which places a lower limit on the degree of anatexis required for a metal-rich magma to separate from its source and ascend through the crust to form a higher-level intrusion. Koopmans et al. (2023) explored melt Li enrichment during a minimum degree partial melting of average shale compositions, for which a starting Li concentration of 125 ppm was assumed. Their modelling predicted that at low-pressure melting, cordierite and biotite were stable, whilst at higher pressures, biotite and muscovite were stable – all of which are potential hosts for Li. Modelling the formation of anatectic pegmatites, Koopmans et al. (2023) calculated that during a single melt cycle, for 7 % partial melting, a maximum enrichment of approximately 4× initial Li could be achieved (Fig. 7). They concluded that it was impossible to generate a melt with sufficient Li content to form Li ore minerals (i.e. 5000 ppm) from the single-stage melting of an ordinary clay protolith. They also highlighted the importance of biotite as perhaps the principal Li host in clay-rich source material. Biotite breakdown releases Li into the melt, but crucially its presence as a restitic mineral acts as a Li sink and serves to inhibit Li melt enrichment. Thus, Koopmans et al. (2023) concluded that in order to form economic LCT pegmatites, either an elevated starting content of Li, or multiple cycles of deep melting were required.

5.3. Fractional crystallization and melt evolution

Granites that are genetically linked to Sn and Li deposits are typically highly fractionated and show evidence of pronounced fluid saturation and hydrothermal activity typically focused in the apical zones of the intrusion (e.g., Cornubian Batholith; Putzolu et al., 2024). Tin (in reducing melts) and lithium are typically incompatible and will further concentrate in residual melt fractions. Progressive crystallization is accompanied by volatile concentration and eventually the exsolution of saline, metal-carrying hydrothermal fluids. The degree of fractionation in mineralized granites is controlled by variables such as magma temperature, initial water content, depth and hence pressure of magma emplacement (Lehmann and Mahawat, 1989).

A limit on the effectiveness of extreme fractionation in generating metal-rich melts is that it becomes increasingly difficult to extract melt from systems beyond 95 % crystallization, since the melt is thought to be effectively locked up within a crystalline mush (Vigneresse et al., 1996). However, Troch et al. (2022) suggested that such crystal frameworks can be disrupted by highly fractionated melts undergoing volatile saturation, such as in the case of pegmatites, and which might provide a mechanism for the melt release even after extreme fractionation.

5.3.1. Mineral chemistry as recorders of melt evolution

Magmatic fractionation is thus key to further concentrating metals, typically monitored through whole rock chemistry using Rb/Sr (e.g., Blevin and Chappell, 1992; Lehmann, 1982; Romer and Kroner, 2016), as well as from mineral chemistry via: zircon and apatite Eu/Eu* (Belousova et al., 2001; Gardiner et al., 2017; Li et al., 2022; Roberts et al., 2024; Sha and Chappell, 1999); La/Yb or Ce/Yb (Azadbakht et al., 2018; Belousova et al., 2001; Chu et al., 2009); Sr/Y (Belousova et al., 2001; Li et al., 2022; O'Sullivan and Chew, 2020); and Mn (Chu et al., 2009; Miles et al., 2014). Minerals with signatures characteristic of extreme fractionation and reducing conditions (e.g., low Eu/Eu*, high Mn) are often found in association with Sn—Li mineralization, consistent with our understanding of Sn—Li metallogeny (Lehmann, 2021). Major and accessory mineral phases saturate and crystallize at different stages during magmatic evolution, so they are a powerful tool to reconstruct magmatic evolution and melt concentrations. However, the use of zircon, apatite and other accessory minerals as tracers of metallogeny during magma fractionation and the magmatic-hydrothermal transition is subject to some caveats.

Firstly, geochemical discriminants such as those mentioned above are often controlled by more than one petrogenetic process. For example, Eu/Eu* in apatite may trace plagioclase fractionation but will also be affected by the oxidation state of the magma (Miles et al., 2014). Similarly, Sr/Y may reflect amphibole fractionation but can also be inherited from the source rock of the magma (Moyen, 2009). Disentangling the respective effects of mineral fractionation, oxidation state,

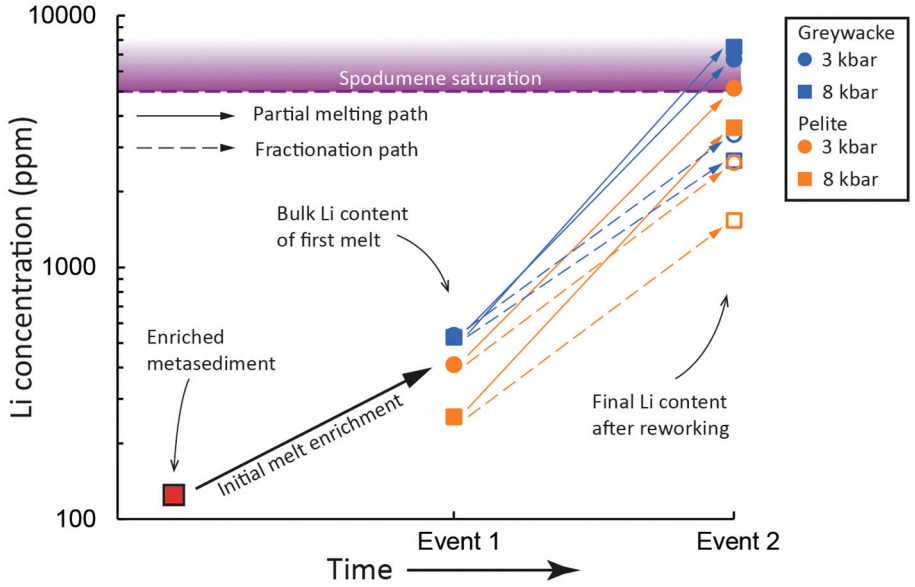


Fig. 7. Evolution of Li concentrations during melting and fractionation of melt components generated during crustal anatexis, from Koopmans et al. (2023). After initial melt extraction, the granite either (1) undergoes fractional crystallization (hollow symbols; the composition of fractional crystallization was taken as the composition at 90 % crystallization); or (2) is assumed to crystallize and then is re-melted and extracted at the 7 % melt threshold (filled shapes).

and source characteristics is difficult but necessary to confidently use geochemical discriminants as redox or fractionation indices.

Secondly, crystal fractionation is unique to each magmatic system, and the compositions of accessory minerals are a function of its relative timing in the crystallization sequence and the crystallizing assemblage. Commonly used geochemical discriminants therefore show significant and overlapping scatter for both barren and mineralized intrusions (Mangler et al., 2024), complicating their utility as pathfinders to mineralization.

Thirdly, modification of mineral compositions via diffusion or metasomatism can obscure primary magmatic signatures. For example, Li is known to be a fast-diffusing element in most rock-forming minerals including apatite and zircon (Audetat et al., 2018; Cherniak and Watson, 2010), which may complicate its petrogenetic interpretation. Similarly, magmatic and hydrothermal fluids may disturb incompatible trace element trends, potentially disrupting primary magmatic signatures (Burnham, 2020; Geisler et al., 2007). For instance, Bouzari et al. (2016) found that hydrothermally altered apatite has a higher Ca and lower trace element concentrations than apatite from unaltered rocks, which they attributed to trace element loss during alteration. This is especially pertinent in magmatic-hydrothermal systems where hot fluids may continue to circulate long after cessation of magmatic activity, perhaps over several millions of years (Robb et al., 2000). However, hydrothermal alteration can often be monitored through textural and geochemical observations: in apatite, monazite and xenotime inclusions indicate alteration by fluids (Harlov, 2015; Harlov et al., 2011). Such disturbance in zircon can be monitored through 'non-stoichiometric' i.e. non-lattice bound elements such as Ca, Fe, and Al which can be involved in substitution during magmatic growth (Hoskin et al., 2000) but which are potentially mobile during later alteration resulting in elevated and variable values that are independent of any magmatic signature (Geisler et al., 2007). In such cases Ca, Fe, and Al abundances should not follow trends linked to magmatic fractionation.

Finally, asserting whether a mineral is of magmatic or hydrothermal origin is often non-trivial. In a classic study of the Sn—W Mole Granite in New South Wales, Pettke et al. (2005) monitored evolving zircon chemistry during a protracted magmatic-hydrothermal transition. They showed that early magmatic zircon had a slight Ce/Ce* anomaly, but as the hydrothermal transition continued, zircon developed an increasingly pronounced Ce/Ce* ratio with correspondingly depleted REE contents, reflecting saturation of other REE bearing minerals such as xenotime and monazite. Li et al. (2014) used zircon REE and Hf contents to discriminate between magmatic versus hydrothermally-derived zircon in complex polymetallic deposits, further linking these to zircon U—Pb ages to assess the relative timing of mineralization events. These authors showed that in their study area Cu (Pb—Zn) mineralization was associated with early granophyric magmas, whilst later W—Sn mineralization with more evolved granite porphyritic intrusions.

5.3.2. *Zircon metal contents*

Contents of Sn, Li and other metals can be measured in many accessory and major minerals, most typically via LA-ICPMS or EPMA, and may prove an effective way of monitoring metal concentration and mobility with the proviso that the mineral phase is considered a reliable recorder of melt or fluid chemistry. Gardiner et al. (2021) explored how metal contents of zircon can monitor Sn mobility during magmatic evolution using a study of the Zaaiplaats tin deposit, Bushveld Complex, South Africa. Zaaiplaats is hosted by the ca. 2.054 Ga A-type Lebowa Granite Suite (LGS) which contains polymetallic (Sn-W-Mo-Cu-Pb-Zn-F) styles of mineralization (Robb et al., 2000). A robust metallogenic model was developed in the 1970s (Groves and McCarthy, 1978) where a single pulse of magma (the Bobbejaankop granite) was extracted from the parental LGS, and which cooled centripetally to reach volatile saturation in the centre, as evidenced by the presence of Sn contents up to 350 ppm (up from 2 to 5 ppm at the margins), disseminated cassiterite, and prominent tourmaline-chlorite-cassiterite rich 'pipes' which cut through the granite (Coetzee and Twist, 1989). Thus, spatially traversing the Bobbejaankop granite conceptually traces through its magmatic history into the magmatic hydrothermal transition. Gardiner et al. (2021) sampled both 'unmineralized' (i.e. background grey granite) and 'mineralized' (from the central mineralized zone) granites, and analyzed separated zircons for trace elements via LA-ICPMS. A 'magmatic baseline' was established by plotting zircon Gd versus Sm (incompatible elements considered fluid immobile) which showed similar trends for both unmineralized or mineralized (Fig. 8A). In contrast, plotting Gd versus Sn showed a clear Sn enrichment in the mineralized samples (Fig. 8C). These data were interpreted as the mineralized samples having experienced elevated concentrations of Sn reflecting its mobility and preferential enrichment in the hydrothermal fluid during vapour saturation. This study illustrates the potential for mineral archives to trace

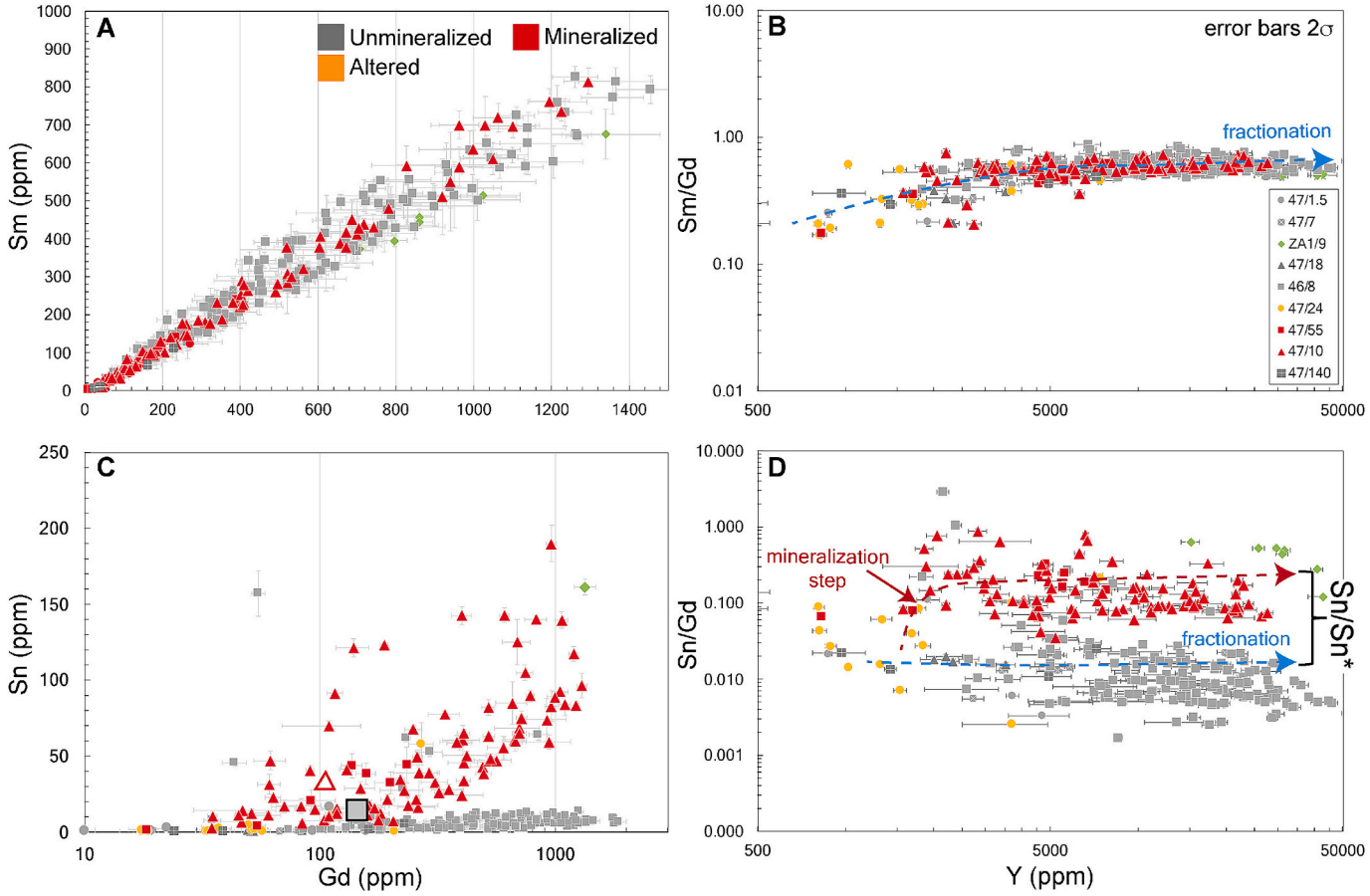


Fig. 8. Zircon trace elements from the Zaaiplaats tin deposit. A,C: Concentrations of Sm & Sn versus Gd, a measure of fractionation. B, D: Plot of zircon Sm/Gd and Sn/Gd versus zircon Y, also a measure of fractionation. The interpreted Zaaiplaats fractionation trend (blue) and mineralization trend (red) are highlighted. D also shows the development of a metal anomaly Sn/Sn*. All plots from Gardiner et al. (2021). Also plotted in A are the whole-rock data as 'zircon equivalent' (using *Kd* values of 10 for Gd (Nardi et al., 2013) and 0.6 for Sn (Pettke et al., 2005)). (For interpretation of the references to colour in this figure legend, the reader is referred to the web version of this article.)

metal concentration during magma evolution, and which is information potentially lost at the whole rock level either via hydrothermal action or later alteration.

5.3.3. *Apatite metal contents*

In addition to zircon, apatite is another ubiquitous accessory mineral whose compositions have been studied with view to exploration. Recently, a small number of studies have examined the use of apatite as a tool to fingerprint Sn mineralization (Azadbakht et al., 2018; Guo et al., 2022; Li et al., 2022). These studies concluded that Mn, Sr, LREE/HREE, and Eu/Eu* are useful geochemical proxies to discriminate between Sn-fertile and barren magmas. However, a compilation of published apatite compositions (Mangler et al., 2024) shows that the scatter and overlap between barren and fertile data is substantial for some proxies (e.g., Mn and La/Yb_N; see Section 5.3.1), rendering them unreliable pathfinders to tin mineralization. On the other hand, the same studies have reported evidence for consistently elevated Sn and Li concentrations in apatite associated with Sn mineralization (Azadbakht et al., 2018; Guo et al., 2022; Li et al., 2022). This suggests that Sn and Li concentrations in apatite may be robust indicators of Sn mineralization (Mangler et al., 2024). If supported by future data, this would call for Li and Sn to be included in apatite trace element analyses, and "face value" metal concentrations in apatite could become reliable pathfinders to tin mineralization.

5.3.4. *Micas and other mineral phases*

Though potentially powerful tracers of Sn-Li-metallogeny, apatite and zircon are accessory minerals that are not major hosts of Li and Sn, and which may not be present at all in some Li—Sn granites. The most common Li hosts in granitoid rocks are micas (Breiter et al., 2023a), including biotite in rhyolitic and phonolitic magmas (Ellis et al., 2022) and Li-rich varieties such as lepidolite, zinnwaldite and polylithionite in extremely fractionated granites and pegmatites (e.g., Černý et al., 1995). Many studies have therefore recently focused on mica compositions to trace magmatic-hydrothermal processes and metal enrichment in granites and pegmatites (Benn et al., 2022; Breiter et al., 2019; Deveaud et al., 2015; Han et al., 2021; Li et al., 2021; Lima et al., 2019; Martins et al., 2012; Putzolu et al., 2024; Zhang et al., 2021). For example, Putzolu et al. (2024) showed that Li-micas are the major hosts of Li, Sn, W, Nb, Ta, and Cs and thus control these metal budgets throughout magmatic and hydrothermal evolution of the Cornubian batholith. On the other hand, Lima et al. (2019) found that spodumene, triphylite and amblygonite (Li-phosphates) in pegmatites in Minas Gerais (Brazil) preferentially fractionate Li, Sn and other metals, leaving micas with lower metal concentrations than those in pegmatites without spodumene and Li-phosphates.

In addition to micas, many other rock-forming and accessory mineral phases in pegmatites have by now been investigated for their potential to trace pegmatite evolution and Li(-Sn-B-Be-Nb-Ta) mineralization, such as tourmaline (Joliff et al., 1986; Lima et al., 2019; Roda-Robles et al., 2015; Roda-Robles et al., 2004); garnet (Hernández-Filiberto et al., 2021; Moretz et al., 2013); columbite-tantalite (Badanina et al., 2015; Melcher et al., 2015; Tindle and Breaks, 2000); monazite-cheralite (Wang et al., 2023); and quartz (Garate-Olave et al., 2017; Keyser et al.,

2023; Müller et al., 2021).

5.3.5. Isotopes as monitors of magma fractionation

Stable Li isotopes can experience significant mass dependent isotope fractionation during both magmatic and hydrothermal processes. The heavier ^{7}Li isotope will be preferentially enriched in the melt over ^{6}Li during magmatic fractionation, making it a useful tracer. Barnes et al. (2012) used δ^{7}Li to monitor magmatic fractionation of rare-element pegmatites of the Little Nahanni Group, New South Wales, and to correlate them with regional, coeval granite intrusions. They documented less evolved pegmatites with relatively low δ^{7}Li that had significant spodumene abundances, and more evolved pegmatites with strong Li isotope fractionation that were typically much more mica-rich and with evidence of significant F enrichment, the latter which they conclude was key for δ^{7}Li fractionation. Similarly, Deveaud et al. (2015) looked at δ^{7}Li variations in muscovite sampled across the pegmatite to infer fractional crystallization extent during crystallization.

Other stable isotopic systems are being investigated as potential useful monitors of magmatic and mineralizing process, and one example is stable Sn isotopes. A recent study on highly evolved Sn mineralizing granites (Sun et al., 2024) showed that Sn isotope ratios (e.g., $\delta^{122/118}$Sn) have the potential to fractionate during, and thus be a monitor of, magma fractionation.

5.4. The magmatic-hydrothermal transition

Volatile exsolution and the associated extraction of metals such as Sn from magmas into hydrothermal fluids is the precursor to the precipitation of hydrothermal ore minerals, and a critical step in the genesis of magmatic-hydrothermal deposits (Burnham, 1979; Candela, 1997; Heinrich, 1990). It has long been considered that Sn preferentially partitions from the silicic melt into the magmatic volatile phase – i.e. the hydrothermal fluid plus volatiles such as CO_2, Cl, F, B etc. derived during volatile saturation. Accordingly, magmatic-hydrothermal Sn deposits were thought to form in response to efficient Sn extraction from the melt upon volatile saturation (Groves and McCarthy, 1978). Recent empirical and experimental studies have assessed the relative timing and composition of hydrothermal fluids and how this affects the efficiency of Sn extraction (Audtat et al., 2000; Zhao et al., 2022b). Some studies have started to dispute the classic model by proposing that Sn remains concentrated within the silicic melt under some circumstances rather than being strongly partitioned into the vapour phase during volatile saturation; Schmidt et al. (2020) explored the partitioning of Sn between melt and hydrothermal fluid at 750 °C as a function of melt aluminium saturation index (ASI), and found that most Sn is preferentially retained in the silicic melt rather than being partitioned into the fluid. Duc-Tin et al. (2007) suggested that Sn partitioning into the hydrothermal fluid was more strongly controlled by the fluid Cl content than F content.

Mineral chemistry can record the magmatic-hydrothermal transition and associated mineralization. In their study of the W—Sn Mole Granite, Pettke et al. (2005) documented both magmatic and hydrothermal zircon and categorized them by their trace element contents. Successive stages of magmatic zircon were characterized by progressive depletion in REE – reflecting the growth of co-existing minerals such as monazite and xenotime. Co-genetic hydrothermal zircon was observed to have similar trace element contents to late-stage magmatic zircon, however a second late-stage hydrothermal zircon was recognized, with distinct trace element zonation, and depletions in Pb and Cs. In their Zaaiplaats study, Gardiner et al. (2021) defined a Sn anomaly (Sn/Sn*; Fig. 8D) the difference between the expected (in response to fractional crystallization) and measured Sn/Gd reflecting an enrichment or depletion of Sn over that from ordinary magmatic fractionation, due to the appearance of a tin-rich hydrothermal fluid. Identification of such mineralization processes in the rock record could provide information on magmatic conditions at that point.

More recently, novel mineral records such as tourmaline have been interrogated to monitor exsolution during magmatic-hydrothermal mineralization. Tourmaline is a common accessory mineral in evolved granitic systems which can saturate both from magmatic and hydrothermal fluids (London and Manning, 1995). Duchoslav et al. (2017) analyzed via LA-ICPMS trace element data in tourmaline from a range of magmatic and hydrothermal deposits in SW England. They documented a range of magmatic and hydrothermal tourmaline, showing that the latter is strongly enriched in Sn and depleted in Ti, Cr, V, and Sc compared to late magmatic tourmaline. In a study of the Ardlethan Sn granite, NSW, Carr et al. (2021) use combined REE and Sn contents of tourmaline to monitor Sn enrichment of some 30× compared to source, and in comparing the tourmaline chemistry to the hosting granite they calculated a $D_{Sn}^{fluid/melt}$ of 0.7.

Biotite has also been investigated as a monitor of volatile saturation. A recent study showed that biotite, which saturates late at relatively low *T* immediately prior to the appearance of a hydrothermal fluid, may trap significant quantities of Li (Ellis et al., 2022) potentially making it a more robust recorder of Li evolution than other co-existing phases.

Tracing the processes of melt evolution and metal partitioning during the magmatic-hydrothermal transition in pegmatites is often problematic, and requires detailed knowledge of mineral paragenesis. The study of the Kamativi pegmatite in Zimbabwe by Shaw et al. (2022) demonstrates that pegmatites are perhaps best thought of as hybrid magmatic-hydrothermal deposits. These workers recognized four distinct paragenetic stages: (1) early magmatic quartz, K-feldspar and spodumene; (2) widespread albitization with cassiterite+columbite growth; (3) development of quartz+muscovite+columbite assemblage; and (4) low-temperature fluid-induced alteration. Likewise, studying the Orange River pegmatite belt in Namaqualand, Namibia, Ballouard et al. (2020) observed that Li-bearing minerals crystallized through the magmatic-hydrothermal transition, and defined three stages: (i) magmatic dominated with spodumene; (ii) an immiscible Li-Cs-Ta rich hydrosaline melt, driving the replacement of the primary mineral assemblage with albite, Li-rich muscovite and zinnwaldite; and (iii) the transition from magmatic to hydrothermal system with Li-Cs-Ta-Bi rich hydrothermal fluids, and the crystallization of lepidolite. It is evident that these systems are characterized by complex and long-lived paragenetic sequences.

5.5. 4D Geodynamics

The importance of biotite breakdown to enrich melt Li and Sn content – as modelled by Koopmans et al. (2023) – implies that deep crustal melting is required to release both Sn and Li, whereas shallow (muscovite-driven) melting will serve to restrict Li enrichment in anatectic melt. These conclusions underline a fundamental requirement that in the absence of a highly enriched source, deep crustal melting of appropriate source rocks is required for economic Li granites and anatectic pegmatites, and this requires a particular tectonic (*P-T*) and hence geodynamic regime.

Similarly, deep crystallization of that melt will serve to precipitate primary spodumene, rather than secondary spodumene having been converted from petalite as SQI. Further, depth of magma evolution and crystallization will play an important role in the timing and nature of volatile exsolution, since the volatile carrying capacity of magmas is highly pressure dependent. Thus, a similar magma composition emplaced at deep versus shallow levels will experience different volatile release timings, processes, and compositions, with ensuing implications for both Sn and Li mobility and mineralization.

A second outcome of this work demonstrates the potential for multi-stage melting as an efficient mechanism for increasing melt Li contents, and the implications of this for the timing of anatectic-origin pegmatite formation in orogenic events. It has long been proposed that multiple melting events are required to 'distill' ever-higher concentrations of incompatible rare metals (e.g., Raimbault et al., 1995). Further, in many pegmatite fields, the pegmatites are often significantly younger than the

spatially-associated granites (Goodenough et al., 2014; Stilling et al., 2006). Recent modelling on Li-bearing granites in the Variscan-aged Massif Central, France supports the idea that remelting of leucocratic orthogneiss is an effective way of forming both Li- and F-enriched melts (Ballouard et al., 2023) – i.e. remelting the crystallized product of an earlier melt cycle (Koopmans et al., 2023). However, an alternative 'multi-stage melt' mechanism to generate metal-rich magmas may be that initial melting of the *source* allows the early removal of low-Sn (and low Li) melts, resulting in a subsequent generation of high-Sn and Li melts to form due to biotite breakdown at deeper melting (e.g., Wolf et al., 2018). Models of multi-stage melting to form enriched granitic melts fit well with the transcrustal view of magmatic systems: ongoing melt generation, ponding, extraction, and evolution over a protracted timescale allows progressive enrichment of metals such as Sn and Li.

Ultimately, these points underline that key to building robust metallogenic models for Sn and Li systems – required for exploration efforts – is constraining the evolving geodynamics which not only serve to drive melting and crystallization processes, but also the geological history leading up to the point of anatexis, which provide the essential ingredients required to form economic deposits. This latter point is especially pertinent if there is a specific requirement for the melt source (e.g., metal pre-enrichment), and hence what geological steps might be required to lead to this (e.g., enhanced weathering in a stable continental interior followed by burial).

5.6. Crustal architecture

The structure of the continental crust at a variety of scales provides pathways for both volatiles and magmas, determines which rock successions are present in the melt zone, and serves to preserve ore deposits. Crustal architecture can be determined geochemically, most successfully using isotope mapping which reveals differing crustal formation ages (Champion, 2013; e.g., Mole et al., 2015), and recent efforts have applied this to tin deposits (Gardiner et al., 2018). Crustal architecture can also control melt ascent. LCT pegmatites are typically emplaced within the upper crust, and transfer of pegmatitic melt from lower crustal levels is thought to be strongly affected by structural lineaments such as fractures or shear zones (Koopmans et al., 2024; Silva et al., 2023). Numerical modelling has recently attempted to model the ascent of anatectic pegmatites (Plunder et al., 2022), building a model of rapid extraction and ascent possibly localized by shear zones.

5.7. Towards a mineral systems model

The development of mineral systems theories over the past three decades (Wyborn et al., 1994) was in part due to the recognition that mineral deposits may have footprints on various scales up to the lithospheric scale, and are commonly clustered in metallogenic provinces with a strong endowment in particular metals (Carlson, 1991). The mineral systems approach combines elements including: lithospheric architecture, geodynamics, sources of metals, and traps (McCuaig and Hronsky, 2014), and links these processes at scale. A goal is therefore to build robust mineral systems models for tin and lithium granitic systems (e.g., Duuring, 2020; M.T. Sweetapple, 2017a, 2017b), especially within the context of a transcrustal model, which can inform new exploration initiatives.

Fig. 9 highlights the critical elements that feed into mineral systems models for Sn—Li granitic deposits: source, favourable geodynamics and crustal architecture, and the depositional environment. We have added constituent elements discussed in this paper, which include: (i) lithosphere architecture, structure and stratigraphy: i.e. what units may melt, where can melts and fluids migrate from and to; (ii) 4D geodynamic and *P-T-t* evolution: what is the evolving melting regime, how does this map to possible source rocks, where will magmas migrate to and crystallize; (iii) Sources of metals, melts and fluids: nature of metal-fertile sedimentary packages, and of pre-enrichment in metals; (iv) depositional

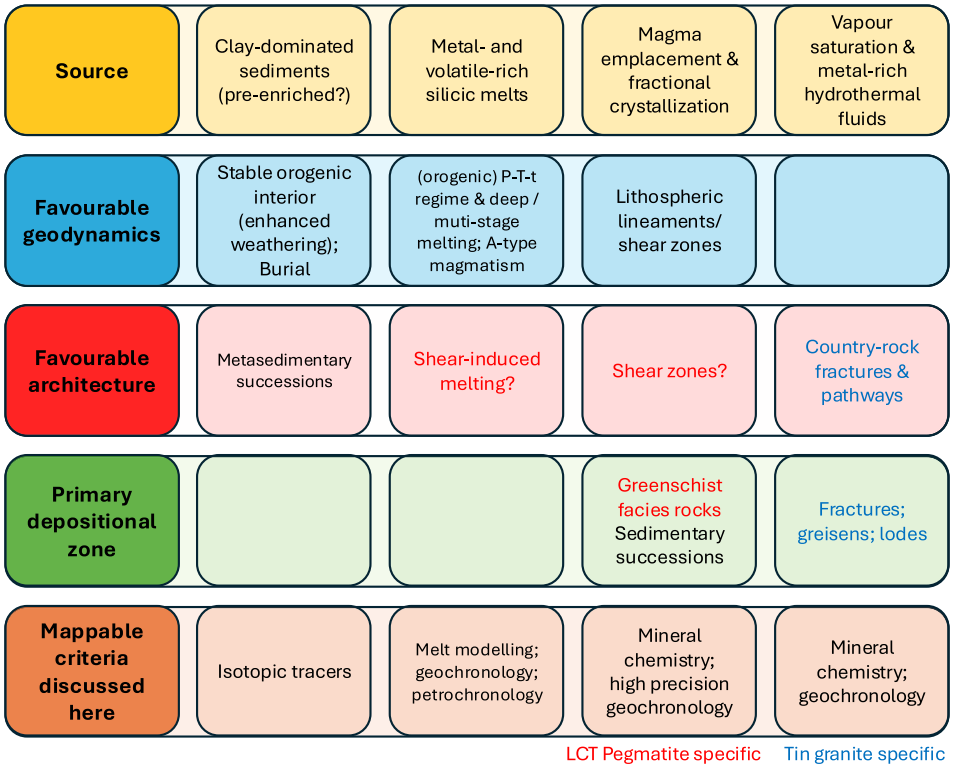


Fig. 9. Critical and constituent elements of Sn—Li mineral systems discussed in this paper, sensu McCuaig and Hronsky (2014); that which applies specifically to tin granites in blue, and to LCT Pegmatites in red. (For interpretation of the references to colour in this figure legend, the reader is referred to the web version of this article.)

mechanisms and zones.

6. Summary and future directions

In this paper we have highlighted current and possible future research directions in tin and lithium metallogeny from a crustal evolution perspective. We have documented examples of the use of mineral chemistry and isotope geochronology coupled with the application of sophisticated thermodynamic melt modelling to constrain magmatic source, the processes of partial melting, the evolution of the melt during fractional crystallization and the onset of vapour saturation and associated metal mobility.

We have outlined key research questions that in our opinion require addressing in future endeavours, and these include:

- Are the ordinary processes of granite formation sufficient to concentrate these metals to form ores? In part, this relates to the ongoing debate around metal pre-enrichment to the magmatic source.
- How are metals kept 'alive' in the system to be concentrated, and not lost to crystallizing phases, or to volatile phases during vapour saturation if magmatic ore minerals are required?
- How do Sn and Li partition between resitic phases and melts, and between silicic melts and fluids, and under what conditions? How sensitive is this latter to, especially, volatile contents and depth?
- What are the timescales of mineralization, and how does the timing (s) of mineralizing events map to the broader evolving magmatic framework?
- For pegmatites, the ongoing debate regarding "last gasp or first sweat" – whether they represent the final fractionated portion of a granite system or low degree crustal melts. How do zoned pegmatite fields fit into these models?
- Transcrustal magmatic system paradigm – can this allow us to view these systems in a different light?
- Can we build robust mineral systems models for tin granites and LCT pegmatites, reconciling the end-member views of pegmatite formation with respect to such models?

To answer these questions, we have outlined some of the current and new approaches, which include:

- New chronometers and tracers, especially with application to pegmatites, where the use of novel isotope tracers such as Rb—Sr in mica, Hf isotopes in cassiterite (Kendall-Langley et al., 2020), or stable Sn isotopes which have the potential monitor both magma fractionation and fluid exsolution (Sun et al., 2024).
- Constraining the timescales of mineralization through new mineral chronometers – e.g. the potential for fluorite via Sm—Nd isochrons (Chesley et al., 1991). More precise ore-forming timescales, e.g. constraining the timescales of whole-lithosphere plumbing processes (Tavazzani et al., 2023) and/or the flux of magma through zircon age distribution (Caricchi et al., 2014).
- Following metal mobility through these systems, especially with the direct measurement of economic metal contents in accessory minerals which may prove a reliable proxy to monitor fluid exsolution, e.g. development of the Sn anomaly (Sn/Sn*) (Gardiner et al., 2021); the use of apatite and other phases to trace volatile evolution (e.g., Stock et al., 2016).
- Application of new melt modelling approaches, including reactive transport models to investigate time- and length-dependent reaction during magma ascent through the crust, and the expansion of current thermodynamic datasets and activity-composition relations to include metals of economic interest and relevant mineral phases.
- Experiments to better derive partitioning information between melt and minerals, and also to constrain the conditions under which metals partition into aqueous fluids.

A better understanding of Sn—Li granite systems, especially within the context of new magmatic paradigms, such as the transcrustal model, can ultimately help build improved metallogenic models for these deposit types and inform new approaches to prospect for them.

Declaration of competing interest

Nick Gardiner and Martin Mangler reports financial support was provided by Leverhulme Trust. Lot Koopmans reports financial support was provided by Natural Environment Research Council. Laurence Robb reports a relationship with Andrada Mining that includes: board membership. If there are other authors, they declare that they have no known competing financial interests or personal relationships that could have appeared to influence the work reported in this paper.

Data availability

No data was used for the research described in the article.

Acknowledgements

We thank Tim Horscroft for the invitation to submit this perspective. NJG and MM thank the Leverhulme Trust for support (Research Project Grant RPG-2023-210). LK was supported by a National Environmental Research Council PhD studentship (Grant no. NE/S007474/1). We thank insightful reviews from Bernard Lehmann and Kathryn Goodenough, and Arturo Gomez-Tuena for editorial handling.

References

Agricola, G., 1556. De re metallica.
Anderson, J.L., 1996. Status of thermobarometry in granitic batholiths. Earth Environ. Sci. Trans. R. Soc. Edinb. 87, 125–138.
Ashworth, L., Kinnaird, J.A., Nex, P.A.M., Harris, C., Müller, A.B., 2020. Origin of rare-element-mineralized Damara Belt pegmatites: a geochemical and light stable isotope study. Lithos 372–373, 105655. https://doi.org/10.1016/j.lithos.2020.105655.
Audetat, A., Zhang, L., Huaiwei, N., 2018. Copper and Li diffusion in plagioclase, pyroxenes, olivine and apatite, and consequences for the composition of melt inclusions. Geochim. Cosmochim. Acta 243, 99–115.
Audtat, A., Gnther, D., Heinrich, C.A., 2000. Magmatic-hydrothermal evolution in a fractionating granite: a microchemical study of the Sn-W-F-mineralized mole granite (Australia). Geochim. Cosmochim. Acta 64, 3373–3393. https://doi.org/10.1016/S0016-7037(00)00428-2.
Azadbakht, Z., Lentz, D.R., McFarlane, C.R.M., 2018. Apatite Chemical Compositions from Acadian-Related Granitoids of New Brunswick, Canada: Implications for Petrogenesis and Metallogenesis. Minerals 8, 598.
Bachmann, O., Bergantz, G.W., 2004. On the origin of crystal-poor rhyolites: extracted from batholithic crystal mushes. J. Petrol. 45, 1565–1582.
Badanina, E.V., Sitnikova, M.A., Gordienko, V.V., Melcher, F., Gäbler, H.E., Lodziak, J., Syritso, L.F., 2015. Mineral chemistry of columbite–tantalite from spodumene pegmatites of Kolmozero, Kola Peninsula (Russia). Ore Geol. Rev. 64, 720–735.
Ballard, J.R., Palin, M.J., Campbell, I.H., 2002. Relative oxidation states of magmas inferred from Ce(IV)/Ce(III) in zircon: application to porphyry copper deposits of northern Chile. Contrib. Mineral. Petrol. 144, 347–364. https://doi.org/10.1007/s00410-002-0402-5.
Ballouard, C., Elburg, M.A., Tappe, S., Reinke, C., Ueckermann, H., Doggart, S., 2020. Magmatic-hydrothermal evolution of rare metal pegmatites from the Mesoproterozoic Orange River pegmatite belt (Namaqualand, South Africa). Ore Geol. Rev. 116, 103252. https://doi.org/10.1016/j.oregeorev.2019.103252.
Ballouard, C., Couzinié, S., Bouilhol, P., Harlaux, M., Mercadier, J., Montel, J.-M., 2023. A felsic meta-igneous source for Li-F-rich peraluminous granites: insights from the Variscan Velay dome (French Massif Central) and implications for rare-metal magmatism. Contrib. Mineral. Petrol. 178, 75. https://doi.org/10.1007/s00410-023-02057-1.
Barnes, E.M., Weis, D., Groat, L.A., 2012. Significant Li isotope fractionation in geochemically evolved rare element-bearing pegmatites from the Little Nahanni Pegmatite Group, NWT, Canada. Lithos 132–133, 21–36. https://doi.org/10.1016/j.lithos.2011.11.014.
Barsukov, V.L., 1957. The geochemistry of tin. Geochemistry 1, 42–52.
Belousova, E.A., Walters, S., Griffin, W.L., O'Reilly, S.Y., 2001. Trace-element signatures of apatites in granitoids from the Mt Isa Inlier, northwestern Queensland. Aust. J. Earth Sci. 48, 603–619.
Belousova, E., Griffin, W., O'Reilly, S.Y., Fisher, N., 2002a. Igneous zircon: trace element composition as an indicator of source rock type. Contrib. Mineral. Petrol. 143, 602–622. https://doi.org/10.1007/s00410-002-0364-7.

Belousova, E., Griffin, W., O'Reilly, S.Y., Fisher, N., 2002b. Apatite as an indicator mineral for mineral exploration: trace-element compositions and their relationship to host rock type. J. Geochem. Explor. 76, 45–69.
Benn, D., Martins, T., Linnen, R.L., 2022. Fractionation and enrichment patterns in white mica from Li pegmatites of the Wekusko Lake Pegmatite Field, Manitoba, Canada. Can. Mineral. 60, 933–956.
Bi, H., Fang, H., Zhang, P., Sudholz, Z., Miller, M.S., Yu, P., Gao, R., 2024. Seismic evidence for a Transcrustal Magmatic Pathway contributing to critical Metal Deposits. Geophys. Res. Lett. 51. https://doi.org/10.1029/2023gl104935.
Blevin, P.L., Chappell, B.W., 1992. The role of magma sources, oxidation states and fractionation in determining the granite metallogeny of eastern Australia. Trans. R. Soc. Edinb. Earth Sci. 83, 305–316.
Blevin, P.L., Chappell, B.W., 1995. Chemistry Origin, and Evolution of Mineralized Granites in the Lachlan Fold Belt, Australia: the Metallogeny of I- and S-Type Granites. Econ. Geol. 90, 1604–1619.
Bouzari, F., Hart, C.J.R., Bissig, T., Barker, S., 2016. Hydrothermal Alteration Revealed by Apatite Luminescence and Chemistry: a potential Indicator Mineral for Exploring Covered Porphyry Copper deposits. Econ. Geol. 111, 1397–1410.
Bowell, R.J., Lagos, L., De Los Hoyos, C.R., Declercq, J., 2020. Classification and Characteristics of Natural Lithium Resources. Elements 16, 259–264. https://doi.org/10.2138/gselements.16.4.259.
Bradley, D., Shea, E., Buchwaldt, R., Bowring, S.A., Benowitz, J., O'Sullivan, P., McCauley, A., 2016. Geochronology and Tectonic Context of Lithium-cesium-tantalum Pegmatites in the Appalachians. Can. Mineral. 54, 945–969.
Breiter, K., Müller, A., Shail, R.K., Simons, B., 2016. Composition of zircons from the Cornubian Batholith of SW England and comparison with zircons from other European Variscan rare-metal granites. Mineral. Mag. 80, 1273–1289.
Breiter, K., Hložková, M., Korbelová, Z., Galiová, M.V., 2019. Diversity of lithium mica compositions in mineralized granite–greisen system: Cínovec Li-Sn-W deposit, Erzgebirge. Ore Geol. Rev. 106, 12–27.
Breiter, K., Galiová, M.V., Korbelová, Z., Hložková, M., 2023a. Can lithium contents in mica be correctly calculated? Tischendorfs proposal (Mineralogical Magazine 61/1997) 25 years after. Mineral. Mag. 87, 878–886.
Breiter, K., Vašinová Galiová, M., Hložková, M., Korbelová, Z., Kynický, J., Costi, H.T., 2023b. Trace element composition of micas from rare-metal granites of different geochemical affiliations. Lithos 446–447, 107135. https://doi.org/10.1016/j.lithos.2023.107135.
Brown, M., Johnson, T.E., Gardiner, N.J., 2020. Plate tectonics and the Archean Earth. Annu. Rev. Earth Planet. Sci. 48, 291–320. https://doi.org/10.1146/annurev-earth-081619-052705.
Bruand, E., Fowler, M., Storey, C., Laurent, O., Antoine, C., Guitreau, M., Heilimo, E., Nebel, O., 2020. Accessory mineral constraints on crustal evolution: elemental fingerprints for magma discrimination. Geochem. Persp. Let. 7–12. https://doi.org/10.7185/geochemlet.2006.
Burnham, C.W., 1979. Magmas and hydrothermal fluids. In: Barnes, H.L. (Ed.), Geochemistry of Hydrothermal Ore Deposits. John Wiley & Sons, pp. 71–136.
Burnham, A.D., 2020. Key concepts in interpreting the concentrations of the rare earth elements in zircon. Chem. Geol. 551. https://doi.org/10.1016/j.chemgeo.2020.119765.
Camacho, A., Baadsgaard, H., Davis, D., Cerny, P., 2012. Radiogenic isotope systematics of the Tanco and Silverleaf granitic pegmatites, Winnipeg river pegmatite district, Manitoba. Can. Mineral. 50, 1775–1792.
Cameron, E.N., Jahns, R.H., McNair, A.H., Page, L.R., 1949. Internal structure of granitic pegmatites. In: Economic Geology Monograph.
Candela, P.A., 1992. Controls on ore metal ratios in granite-related ore systems: an experimental and computational approach. Trans. R. Soc. Edinb. Earth Sci. 83, 317–326.
Candela, P.A., 1997. A Review of Shallow, Ore-related Granites: Textures, Volatiles, and Ore Metals. J. Petrol. 38, 1619–1633.
Caricchi, L., Simpson, G., Schaltegger, U., 2014. Zircons reveal magma fluxes in the Earth's crust. Nature 511, 457–461.
Carlson, C.A., 1991. Spatial distribution of ore deposits. Geology 19, 111–114.
Carr, P.A., Norman, M.D., Bennett, V.C., 2017. Assessment of crystallographic orientation effects on secondary ion mass spectrometry (SIMS) analysis of cassiterite. Chem. Geol. 467, 122–133.
Carr, P., Norman, M.D., Bennett, V.C., Blevin, P.L., 2021. Tin Enrichment in Magmatic-Hydrothermal Environments Associated with Cassiterite Mineralization at Ardlethan, Eastern Australia: Insights from Rb-Sr and Sm-Nd Isotope Compositions in Tourmaline. Econ. Geol. 116, 147–167. https://doi.org/10.5382/econgeo.4774.
Cashman, K.V., Sparks, R.S.J., Blundy, J., 2017. Vertically extensive and unstable magmatic systems: a unified view of igneous processes. Science 355.
Cawood, P.A., Hawkesworth, C.J., 2015. Temporal relations between mineral deposits and global tectonic cycles. Geol. Soc. Lond. Spec. Publ. 393, 9–21. https://doi.org/10.1144/sp393.1.
Cawood, P.A., Kröner, A., Collins, W.J., Kusky, T.M., Mooney, W.D., Windley, B.F., 2009. Accretionary orogens through Earth history. Geol. Soc. Lond. Spec. Publ. 318, 1–36.
Cawood, P.A., Hawkesworth, C.J., Dhuime, B., 2013. The continental record and the generation of continental crust. Geol. Soc. Am. Bull. 125, 14–32. https://doi.org/10.1130/b30722.1.
Cawood, P.A., Hawkesworth, C., Pisarevsky, S.A., Dhuime, B., Capitanio, F.A., Nebel, O., 2018. Geological archive of the onset of plate tectonics. Philos. Trans. A Math. Phys. Eng. Sci. 376. https://doi.org/10.1098/rsta.2017.0405.
Černý, P., 1991a. Rare-element granitic pegmatites. part II: Regional to global environments and petrogenesis. Geosci. Can. 18, 68–81.
Černý, P., 1991b. Rare-element granitic pegmatites. Part I: anatomy and internal evolution of pegmatitic deposits. Geosci. Can. 18, 49–67.
Černý, P., 1992. Geochemical and petrogenetic features of mineralization in rare-element granitic pegmatites in the light of current research. Appl. Geochem. 7, 393–416.
Cerny, P., Siivola, J., 1980. The Tanco Pegmatite at Bernic Lake, Manitoba; XII, Hafnian Zircon. Can. Mineral. 18, 313–321.
Černý, P., Staněk, J., Novák, M., Baadsgaard, H., Rieder, M., Ottolini, L., Kavalová, M., Chapman, R., 1995. Geochemical and structural evolution of micas in the Rožná and Dobrá Voda pegmatites, Czech Republic. Mineral. Petrol. 55, 177–201.
Černý, P., Blevin, P.L., Cuney, M., London, D., 2005. Granite-related ore deposits. In: Hedenquist, J.W., Thompson, J.F.H., Goldfarb, R.J., Richards, J.P. (Eds.), Economic Geology 100th Anniversary Volume. Society of Economic Geologists, pp. 337–370.
Champion, D.C., 2013. Neodynium Depleted Mantle Model Age Map of Australia. Geoscience Australia, Canberra.
Chappell, B.W., White, A.J.R., 2001. Two contrasting granie types: 25 years later. Aust. J. Earth Sci. 48, 489–499.
Che, X.D., Wu, F.-Y., Wang, R.-C., Gerdes, A., Ji, W.-Q., Zhao, Z.-H., Yang, J.-H., Zhu, Z.-Y., 2015. In situ U–Pb isotopic dating of columbite–tantalite by LA–ICP–MS. Ore Geol. Rev. 65, 979–989.
Chelle-Michou, C., Rottier, B., 2021. Transcrustal magmatic controls on the size of porphyry Cu systems: state of knowledge and open questions. Econ. Geol. Spe. Publ. 24, 87–100.
Cheng, Y., Spandler, C., Kemp, A.I., Mao, J., Rusk, B., Hu, Y., Blake, K., 2019. Controls on Cassiterite (SnO2) Crystallization: evidence from Cathodoluminescence, Trace-Element Chemistry, and Geochronology at the Gejiu Tin District. Am. Mineral. 104, 118–129.
Cherniak, D.J., 2010. Diffusion in Accessory Minerals: Zircon, Titanite, Apatite, Monazite and Xenotime. Rev. Mineral. Geochem. 72, 827–869.
Cherniak, D.J., Watson, E.B., 2010. Li diffusion in zircon. Contrib. Mineral. Petrol. 160, 383–390.
Chesley, J.T., Halliday, A.N., Scrivener, R.C., 1991. Samarium-Neodymium Direct Dating of Fluorite Mineralization. Science 252, 949–951.
Chhibber, H.L., 1934. The Mineral Resources of Burma. Macmillan and Co, London.
Chu, M.-F., Wang, K.-L., Griffin, W.L., Chung, S.L., O'Reilly, S.Y., Pearson, N.J., Iizuka, Y., 2009. Apatite Composition: Tracing Petrogenetic Processes in Transhimalayan Granitoids. J. Petrol. 50, 1829–1855.
Cobbing, E.J., Mallick, D.I.J., Pitfield, P.E.J., Teoh, L.H., 1986. The granites of the Southeast Asian Tin Belt. J. Geol. Soc. Lond. 143, 537–550.
Coetzee, J., Twist, D., 1989. Disseminated Tin Mineralization in the Roof of the Bushveld Granite Pluton at the Zaaiplaats Mine, with Implications for the Genesis of Magmatic Hydrothermal Tin Systems. Econ. Geol. 84, 1817–1834.
Copley, A., Weller, O.M., 2022. The controls on the thermal evolution of continental mountain ranges. J. Metamorph. Geol. 40, 1235–1270.
Coward, M.P., 1990. The Precambrian, Caledonian and Variscan framework to NW Europe. Geol. Soc. Lond. Spec. Publ. 55, 1–34.
Darbyshire, D., Shepherd, T.J., 1994. Nd and Sr isotope constraints on the origin of the Cornubian batholith, SW England. J. Geol. Soc. Lond. 151, 795–802.
Deveaud, S., Millot, R., Villaros, A., 2015. The genesis of LCT-type granitic pegmatites, as illustrated by lithium isotopes in micas. Chem. Geol. 411, 97–111. https://doi.org/10.1016/j.chemgeo.2015.06.029.
Dilles, J.H., Kent, A.J.R., Wooden, J.L., Tosdal, R.M., Koleszar, A., Lee, R.G., Farmer, L.P., 2015. Zircon compositional evidence for sulfur-degassing from ore-forming magmas. Econ. Geol. 110, 241–251.
Ding, T., Ma, D., Zhang, R., 2015. Apatite in granitoids related to polymetallic mineral deposits in southeastern Hunan Province, Shi–Hang zone, China: Implications for petrogenesis and metallogenesis. Ore Geol. Rev. 69, 104–117.
Dittrich, T., Seifert, T., Schulz, B., Hagemann, S., Gerdes, A., Pfänder, J., 2019a. Introduction to Archean rare-metal pegmatites. In: Archean Rare-Metal Pegmatites in Zimbabwe and Western Australia. Springer.
Dittrich, T., Seifert, T., Schulz, B., Hagemann, S.G., Gerdes, A., Pfänder, J., 2019b. Archean Rare-Metal Pegmatites in Zimbabwe and Western Australia. Springer.
Duchoslav, M., Marks, M.A.W., Drost, K., McCammon, C., Marschall, H.R., Wenzel, T., Markl, G., 2017. Changes in tourmaline composition during magmatic and hydrothermal processes leading to tin-ore deposition: the Cornubian Batholith, SW England. Ore Geol. Rev. 83, 215–234.
Duc-Tin, Q., Audétat, A., Keppler, H., 2007. Solubility of tin in (Cl, F)-bearing aqueous fluids at 700°C, 140MPa: a LA-ICP-MS study on synthetic fluid inclusions. Geochim. Cosmochim. Acta 71, 3323–3335. https://doi.org/10.1016/j.gca.2007.04.022.
Duuring, P., 2020. Rare-Element Pegmatites: A Mineral Systems Analysis. Geological Survey of Western Australia, East Perth, Western Australia.
Edmonds, M., Cashman, K.V., Holness, M., Jackson, M., 2019. Architecture and dynamics of magma reservoirs. Philos. Trans. A Math. Phys. Eng. Sci. 377, 20180298. https://doi.org/10.1098/rsta.2018.0298.
Ellis, B.S., Neukampf, J., Bachmann, O., Harris, C., Forni, F., Magna, T., Laurent, O., Ulmer, P., 2022. Biotite as a recorder of an exsolved Li-rich volatile phase in upper-crustal silicic magma reservoirs. Geology 50, 481–485.
Farges, F., Linnen, R.L., Brown, G.E., 2006. Redox and Speciation of tin in hydrous silicate glasses: a comparison with Nb, Ta, Mo and W. Can. Mineral. 44, 795–810. https://doi.org/10.2113/gscanmin.44.3.795.
Floyd, P.A., Exley, C.S., Styles, M.T., 1993. The Cornubian granite batholith(Group C sites). In: Floyd, P.A., Exley, C.S., Styles, M.T. (Eds.), Igneous Rocks of South-West England. Springer, pp. 141–208.
Fuchsloch, W.C., Nex, P.A.M., Kinnaird, J.A., 2018. Classification, mineralogical and geochemical variations in pegmatites of the Cape Cross-Uis pegmatite belt, Namibia. Lithos 296–299, 79–95. https://doi.org/10.1016/j.lithos.2017.09.030.
Garate-Olave, I., Müller, A., Roda-Robles, E., Gil-Crespo, P.P., Pesquera, A., 2017. Extreme fractionation in a granite–pegmatite system documented by quartz

chemistry: the case study of Tres Arroyos (Central Iberian Zone, Spain). Lithos 286, 162–174.
Gardiner, N.J., Searle, M.P., Robb, L.J., Morley, C.K., 2015a. Neo-Tethyan magmatism and metallogeny in Myanmar – an Andean analogue? J. Asian Earth Sci. 106, 197–215. https://doi.org/10.1016/j.jseaes.2015.03.015.
Gardiner, N.J., Sykes, J.P., Trench, A., Robb, L.J., 2015b. Tin mining in Myanmar: production and potential. Res. Policy 46, 219–233. https://doi.org/10.1016/j.resourpol.2015.10.002 rsus gere.
Gardiner, N.J., Hawkesworth, C.J., Robb, L.J., Whitehouse, M.J., Roberts, N.M., Kirkland, C.L., Evans, N.J., 2017. Contrasting granite metallogeny through the zircon record: a case study from Myanmar. Sci. Rep. 7, 748. https://doi.org/10.1038/s41598-017-00832-2.
Gardiner, N.J., Searle, M.P., Morley, C.K., Robb, L.J., Whitehouse, M.J., Roberts, N.M.W., Kirkland, C.L., Spencer, C.J., 2018. The crustal architecture of Myanmar imaged through zircon U-Pb, Lu-Hf and O isotopes: Tectonic and metallogenic implications. Gondwana Res. 62, 27–60. https://doi.org/10.1016/j.gr.2018.02.008.
Gardiner, N.J., Hawkesworth, C., Robb, L.J., Mulder, J.A., Wainwright, A.N., Cawood, P. A., 2021. Metal anomalies in zircon as a record of granite-hosted mineralization. Chem. Geol. 585, 120580. https://doi.org/10.1016/j.chemgeo.2021.120580.
Gardiner, N.J., Mulder, J.A., Szilas, K., Nebel, O., Whitehouse, M., Jeon, H., Cawood, P. A., 2023a. A record of Neoarchaean cratonisation from the Storø Supracrustal Belt, West Greenland. Earth Planet. Sci. Lett. 602. https://doi.org/10.1016/j.epsl.2022.117922.
Gardiner, N.J., Roberts, J.J., Johnson, G., Smith, D.J., Bond, C.E., Knipe, R., Haszeldine, S., Gordon, S., O'Donnell, M., 2023b. Geosciences and the energy transition. Earth Sci. Syst. Soc. 3, 10072. https://doi.org/10.3389/esss.2023.10072.
Gardiner, N.J., Jowitt, S.M., Sykes, J.P., 2024. Lithium: critical, or not so critical? Geoenergy 2. https://doi.org/10.1144/geoenergy2023-045.
Geisler, T., Schaltegger, U., Tomaschek, F., 2007. Re-equilibration of Zircon in Aqueous Fluids and Melts. Elements 3, 43–50. https://doi.org/10.2113/gselements.3.1.43.
Glorie, S., Simpson, A., Gilbert, S.E., Hand, M., Müller, A., 2024. Testing the reproducibility of in situ Lu-Hf dating using Lu-rich garnet from the Tørdal pegmatites, southern Norway. Chem. Geol. 122038.
Goodenough, K.M., Lusty, P.A.J., Roberts, N.M.W., Key, R.M., Garba, A., 2014. Post-collisional Pan-African granitoids and rare metal pegmatites in western Nigeria: Age, petrogenesis, and the 'pegmatite conundrum'. Lithos 200–201, 22–34. https://doi.org/10.1016/j.lithos.2014.04.006.
Goodey, M.A., Tapster, S., Roberts, N.M.W., Gardiner, N.J., Robb, L.J., Shail, R.K., Bista, D., 2023. Turning Advances in High-Precision Cassiterite U-Pb Geochronology into Improved Mineral System Models. Presented at the Goldschmidt, Lyon.
Green, E.C.R., White, R.W., Diener, J.F.A., Powell, R., Holland, T.J.B., Palin, R.M., 2016. Activity-composition relations for the calculation of partial melting equilibria in metabasic rocks. J. Metamorph. Geol. 34, 845–869. https://doi.org/10.1111/jmg.12211.
Groves, D.I., 1972. The Geochemical Evolution of Tin-Bearing Granites in the Blue Tier Batholith, Tasmania. Econ. Geol. 67, 445–457.
Groves, D.I., Bierlein, F.P., 2007. Geodynamic settings of mineral deposit systems. J. Geol. Soc. Lond. 164, 19–30. https://doi.org/10.1144/0016-76492006-065.
Groves, D.I., McCarthy, T.S., 1978. Fractional crystallization and the origin of tin deposits in granitoids. Mineral. Deposita 13, 11–26.
Guaida, G.A., Ghiorso, M.S., Lemons, R.V., Carley, T.L., 2012. Rhyolite-MELTS: a modified calibration of MELTS optimized for silica-rich, fluid-bearing magmatic systems. J. Petrol. 53, 875–890.
Guimarães, F.S., de Oliveira, A.L.R., Amorim, L.E.D., Rios, F.J., Lehmann, B., Hernández, C.R., Moraes, R., 2021. Lithium-mica composition as pathfinder and recorder of Grenvillian-age greisenization, Rondonia Tin Province, Brazil. Geochemistry 81, 125737.
Gulson, B.L., Jones, M.T., 1992. Cassiterite: potential for direct dating of mineral deposits and a precise age for the Bushveld Complex granites. Geology 20, 355–358.
Guo, J., Zhang, G., Xiang, L., Zhang, R., Zhang, L., Sun, W., 2022. Combined mica and apatite chemical compositions to trace magmatic-hydrothermal evolution of fertile granites in the Dachang Sn-polymetallic district, South China. Ore Geol. Rev. 151, 105168.
Han, J., Chen, H., Hollings, P., Wang, J., Zhang, D., Zhang, L., Zeng, T., Ma, J., Ai, Y., 2021. Efficient enrichment of Rb during the magmatic-hydrothermal transition in a highly evolved granitic system: Implications from mica chemistry of the Tiantangshan Rb-Sn-W deposit. Chem. Geol. 260, 120020.
Harlov, D.E., 2015. Apatite: a Fingerprint for Metasomatic Processes. Elements 11, 171–176.
Harlov, D.E., Wirth, R., Hetherington, C.J., 2011. Fluid-mediated partial alteration in monazite: the role of coupled dissolution–reprecipitation in element redistribution and mass transfer. Contrib. Mineral. Petrol. 162, 329–348.
Hart, C.J.R., Mair, J.L., Goldfarb, R.J., Groves, D.I., 2004. Source and redox controls on metallogenic variations in intrusion-related ore systems, Tombstone-Tungsten Belt, Yukon Territory, Canada. Trans. R. Soc. Edinb. Earth Sci. 95, 339–356.
Hawkesworth, C.J., Gallagher, K., Hergt, J.M., McDermott, F., 1993. Mantle and slab contributions in arc magmas. Annu. Rev. Earth Planet. Sci. 21, 175–204.
Hedenquist, J.W., Lowenstein, J.B., 1994. The role of magmas in the formation of hydrothermal ore deposits. Nature 370, 519–527.
Heinonen, J.S., Bohrson, W.A., Spera, F.J., Brown, G.A., Scruggs, M.A., Adams, J.V., 2020. Diagnosing open-system magmatic processes using the Magma Chamber Simulator (MCS): part II—trace elements and isotopes. Contrib. Mineral. Petrol. 175, 1–21.
Heinrich, C., 1990. The Chemistry of Hydrothermal Tin (−Tungsten) Ore Deposition. Econ. Geol. 85, 457–481.
Helz, R.T., 1976. Phase Relations of Basalts in their Melting Ranges at PH2O = 5 kb. Part II. Melt Compositions. J. Petrol. 17, 139–193.
Hernández-Filiberto, L., Roda-Robles, E., Simmons, W.B., Webber, K.L., 2021. Garnet as indicator of pegmatite evolution: the case study of pegmatites from the Oxford Pegmatite Field (Maine, USA). Minerals 11, 802.
Hetherington, C.J., Mailloux, G.A., Miller, B.V., 2021. A multi-mineral U-(Th)-Pb dating study of the Stetind pegmatite of the Tysfjord region, Norway, and implications for production of NYF-rare element pegmatites during orogenic collapse. Lithos 398–399, 106257.
Hoskin, P.W.O., 2003. The Composition of Zircon and Igneous and Metamorphic Petrogenesis. Rev. Mineral. Geochem. 53, 27–62. https://doi.org/10.2113/0530027.
Hoskin, P.W.O., Kinny, P.D., Wyborn, D., Chappell, B.W., 2000. Identifying accessory mineral saturation during differentiation in granitoid magmas: an integrated approach. J. Petrol. 41, 1365–1396.
Hulsbosch, N., Muchez, P., 2020. Tracing Fluid Saturation during Pegmatite Differentiation by Studying the Fluid Inclusion Evolution and Multiphase Cassiterite Mineralisation of the Gatumba Pegmatite Dyke System (NW Rwanda). Lithos 354–355, 105285.
Humboldt, A., 1823. Essai géognostique Sur le Gisement Des Roches Dans les Deux hemisphères. Levrault, Strasbourg.
Hutchison, C.S., 1977. Granite emplacement and tectonic subdivision in Peninsular Malaysia. Geol. Soc. Malaysia Bull. 9, 198–207.
IEA, 2022. The Role of Critical Minerals in Clean Energy Transitions, World Energy Outlook Special Report. International Energy Agency (IEA), Paris.
Imayama, T.T.K.M.R., Takeshita, T., Yi, K., Fukuyama, M., 2019. Early Oligocene partial melting via biotite dehydration melting and prolonged low-pressure–low-temperature metamorphism of the upper High Himalaya Crystalline Sequence in the far east of Nepal. Geol. Soc. Lond. Spec. Publ. 481, 147–173.
Ishihara, S., 1981. The granitoid series and mineralization. In: Economic Geology 75th Anniversary, 458–484.
Jackson, N.J., Willis-Richards, J., Manning, D.A.C., Sams, M.S., 1989. Evolution of the Cornubian Ore Field, Southwest England: Part II. Mineral Deposits and Ore-Forming Processes. Econ. Geol. 84, 1101–1133.
Jackson, M.D., Blundy, J., Sparks, R.S.J., 2018. Chemical differentiation, cold storage and remobilization of magma in the Earth's crust. Nature 564, 405–409.
Jacobson, M., 2007. Guidebook to the Pegmatites of Western Australia. Hesperian Press, Carlisle/Western Australiaj.
Jahns, R.H., 1953. The genesis of pegmatites: 1. Occurrence and origin of giant crystals. Am. Mineral. 38, 563–598.
Jahns, R.H., 1955. The Study of Pegmatites Deposits. In: Economic Geology 50th Anniversary Volume. Society of Economic Geologists.
Joliff, B.L., Papike, J.J., Shearer, C.K., 1986. Tourmaline as a recorder of pegmatite evolution; Bob Ingersoll pegmatite, Black Hills, South Dakota. Am. Mineral. 71, 472–500.
Jowitt, S., McNulty, B., 2021. Battery and energy metals: Future drivers of the minerals industry? SEG Discov. 127, 11–18.
Kaeter, D., Barros, R., Mengue, J., Chew, D.M., 2018. The Magmatic–hydrothermal transition in Rare-Element Pegmatites from Southeast Ireland: LA-ICP-MS Chemical Mapping of Muscovite and Columbite–tantalite. Geochim. Cosmochim. Acta 240, 98–130.
Kaeter, D., Barros, R., Mengue, J., 2021. Metasomatic High Field Strength Element, Tin, and Base Metal Enrichment Processes in Lithium Pegmatites from Southeast Ireland. Econ. Geol. 116, 169–198.
Kelsey, D.E., Powell, R., 2011. Progress in linking accessory mineral growth and breakdown to major mineral evolution in metamorphic rocks: a thermodynamic approach in the Na2O-CaO-K2O-FeO-MgO-Al2O3-SiO2-H2O-TiO2-ZrO2 system. J. Metamorph. Geol. 29, 151–166.
Kemp, A.I., Hawkesworth, C., 2013. Granitic Perspectives on the Generation and Secular Evolution of the Continental Crust. In: Holland, H., Turekian, K. (Eds.), Treatise on Geochemistry. Elsevier, pp. 349–421.
Kemp, A.I.S., Hawkesworth, C.J., 2014. Growth and differentiation of the continental crust from isotope studies of accessory minerals. In: Treatise on Geochemistry, 2nd ed. Elsevier, pp. 379–421.
Kemp, A.I., Hawkesworth, C.J., Foster, G.L., Paterson, B.A., Woodhead, J.D., Hergt, J.M., Gray, C.M., Whitehouse, M.J., 2007. Magmatic and crustal differentiation history of granitic rocks from Hf-O isotopes in zircon. Science 315, 980–983. https://doi.org/10.1126/science.1136154.
Kendall-Langley, L.A., Kemp, A.I.S., Grigson, J.L., Hammerli, J., 2020. U-Pb and reconnaissance Lu-Hf isotope analysis of cassiterite and columbite group minerals from Archean Li-Cs-Ta type pegmatites of Western Australia. Lithos 352–353. https://doi.org/10.1016/j.lithos.2019.105231.
Kerrich, R., Goldfarb, R.J., Richards, J.P., 2005. Metallogenic provinces in an evolving geodynamic framework. In: Economic Geology 110th Anniversary Edition, pp. 1097–1136.
Keyser, W., Müller, A., Knoll, T., Mengue, J., Steiner, R., Berndt, J., Hart, E., Fegan, T., Harrop, J., 2023. Quartz chemistry of lithium pegmatites and its petrogenetic and economic implications: examples from Wolfsberg (Austria) and Moylisha (Ireland). Chem. Geol. 630, 121507.
Kinnaird, J., Bowden, P., 1987. African Anorogenic Alkaline Magmatism and Mineralization—a Discussion with Reference to the Niger-Nigeria Province. Geol. J. 22, 279–340.
Kinnaird, J.A., Nex, P.A.M., Milani, L., 2016. Tin in Africa. Episodes 39, 361–380. https://doi.org/10.18814/epiiugs/2016/v39i2/95783.
Kinny, P.D., 2000. U-Pb dating of rare-metal (Sn-Ta-Li) mineralized pegmatites in Western Australia by SIMS analysis of tin and tantalum-bearing ore minerals. In: Beyond 2000, New Frontiers in Isotope Geoscience, pp. 113–116.

Kontak, D.J., Creaser, R.A., Heaman, L.M., Archibald, D.A., 2005. U-Pb tantalite, Re-Os molybdenite, and 40Ar/39Ar muscovite dating of the Brazil Lake pegmatite, Nova Scotia: a possible shear-zone related origin for an LCT-type pegmatite. Atlantic Geoscience 41.

Koopmans, L., Martins, T., Linnen, R., Gardiner, N.J., Breasley, C.M., Palin, R.M., Groat, L.A., Silva, D., Robb, L.J., 2023. The formation of lithium-rich pegmatites through multi-stage melting. Geology. https://doi.org/10.1130/g51633.1.

Koopmans, L., St Pierre, B., Palin, R.M., Gardiner, N.J., Robb, L.J., 2024. Structural controls on the emplacement and mineralization of lithium-bearing pegmatites. In: Presented at the GAC-MAC-PEG 2024, Brandon, Manitoba.

Kruger, F.J., Kamber, B.S., Harris, P.A., 1998. Isotopic peculiarities of an Archaean pegmatite (Union Mine, Mica, South Africa): Geochemical and geochronological implications. Precambrian Res. 91, 253–267.

Kunz, B.E., Warren, C.J., Jenner, F.E., Harris, N.B.W., Argles, T.W., 2022. Critical metal enrichment in crustal melts: the role of metamorphic mica. Geology 50, 1219–1223. https://doi.org/10.1130/g50284.1.

Laurent, O., Martin, H., Moyen, J.F., Doucelance, R., 2014. The diversity and evolution of late-Archean granitoids: evidence for the onset of "modern-style" plate tectonics between 3.0 and 2.5 Ga. Lithos 205, 208–235.

Legros, H., Marignac, C., Mercadier, J., Cuney, M., Richard, A., Wang, R.-C., Charles, N., Lespinasse, M.-Y., 2016. Detailed paragenesis and Li-mica compositions as recorders of the magmatic-hydrothermal evolution of the Maoping W-Sn deposit (Jiangxi, China). Lithos 264, 108–124.

Legros, H., Mercadier, J., Villeneuve, J., Romer, R.L., Deloule, E., Van Lichtervelde, M., Dewaele, S., Lach, P., Che, X.-D., Wang, R.-C., Zhu, Z.-Y., Gloaguen, E., Melleton, J., 2019. U-Pb isotopic dating of columbite-tantalite minerals: Development of reference materials and in situ applications by ion microprobe. Chem. Geol. 512, 69–84. https://doi.org/10.1016/j.chemgeo.2019.03.001.

Lehmann, B., 1982. Metallogeny of Tin: Magmatic Differentiation versus Geochemical Heritage. Econ. Geol. 77, 50–59.

Lehmann, B., 1990. The Metallogeny of Tin. Springer, Berlin.

Lehmann, B., 2021. Formation of tin ore deposits: a reassessment. Lithos 402–403, 105756. https://doi.org/10.1016/j.lithos.2020.105756.

Lehmann, B., Mahawat, C., 1989. Metallogeny of tin in central Thailand: a genetic concept. Geology 17, 426–429.

Leopardi, D., Gerdes, A., Albert, R., Gutzmer, J., Lehmann, B., Burisch, M., 2024. LA-ICP-MS U-Pb cassiterite age data of the Sadisdorf deposit link Sn-Li-(W-Cu) mineralization in the eastern Erzgebirge to the collapse of the Altenberg-Teplice Caldera. Geochemistry 84, 126038.

Li, H., Watanabe, K., Yonezu, K., 2014. Zircon morphology, geochronology and trace element geochemistry of the granites from the Huangshaping polymetallic deposit, South China: Implications for the magmatic evolution and mineralization processes. Ore Geol. Rev. 60, 14–35. https://doi.org/10.1016/j.oregeorev.2013.12.009.

Li, X., Gao, Q., Song, H., Chi, G., Lai, C.-K., 2019. Discriminating ore fertile and barren granites using zircon Ce and Eu anomalies – Perspective from late Mesozoic (Yanshanian) granites in South China. Ore Geol. Rev. 113. https://doi.org/10.1016/j.oregeorev.2019.103105.

Li, P., Chen, Z., Liu, X., Huang, Z., Zhou, F., 2021. Compositional evolution of the muscovite of Renli pegmatite-type rare-metal deposit, Northeast Hunan, China: Implications for its petrogenesis and mineralization potential. Ore Geol. Rev. 138, 104380.

Li, J., Chen, S.-Y., Zhao, Y.-H., 2022. Trace elements in apatite from Gejiu Sn polymetallic district: Implications for petrogenesis, metallogenesis and exploration. Ore Geol. Rev. 145, 104880. https://doi.org/10.1016/j.oregeorev.2022.104880.

Lima, J.L., Scholz, R., Lana, C., Queiroga, G., 2019. Mica and tourmaline geochemistry of pegmatites from Conselheiro Pena Pegmatite District, Minas Gerais, Brazil: Implications for pegmatite genesis and economic potential. Geochem. J. 53, 151–170.

Linnen, R.L., 1996. The combined effects of fO2 and melt composition on SnO2 solubility and tin diffusivity in haplogranitic melts. Geochim. Cosmochim. Acta 60, 4965–4976.

Linnen, R.L., 1998. The Solubility of Nb-Ta-Zr-Hf-W in Granitic Melts with Li and Li + F: Constraints for Mineralization in rare Metal Granites and Pegmatites. Econ. Geol. 93, 1013–1025.

Linnen, R.L., Keppler, H., 2002. Melt composition control of Zr/Hf fractionation in magmatic processes. Geochim. Cosmochim. Acta 66, 3293–3301.

Linnen, R.L., Van Lichtervelde, M., Cerny, P., 2012. Granitic pegmatites as sources of strategic metals. Elements 8, 275–280.

London, D., 1984. Experimental phase equilibria in the system LiAlSiO4–SiO2–H2O: a petrogenetic grid for lithiumx-rich pegmatites. Am. Mineral. 69, 995–1004.

London, D., 1986. Magmatic-Hydrothermal transition in the Tanco Rare-Element Pegmatite: evidence from Fluid Inclusions and Phase-Equilibrium experiments. Am. Mineral. 71, 376–395.

London, D., 2008. Pegmatites. The Canadian Mineralogist Special Publication.

London, D., 2014. A petrologic assessment of internal zonation in granitic pegmatites. Lithos 184–187, 74–104.

London, D., 2018. Ore-Forming Processes within Granitic Pegmatites. Ore Geol. Rev. 101, 349–383.

London, D., Manning, D.A.C., 1995. Chemical variation and significance of tourmaline from Southwest England. Econ. Geol. 90, 495–519.

London, D., Morgan, G.B., 1996. Boron in granitic rocks and their contact aureoles. In: Boron: Mineralogy, Petrology and Geochemistry, Reviews in Mineralogy. Mineralogical Society of America, pp. 299–330.

London, D., Morgan, G.B., 2017. Experimental Crystallization of the Macusani Obsidian, with applications to Lithium-Rich Granitic Pegmatites. J. Petrol. 58, 1005–1030.

Lu, Y.J., Loucks, R.R., Fiorentini, M.L., McCuaig, T.C., Evans, N.J., Yang, Z.M., Hou, Z.Q., Kirkland, C.L., Parra-Avila, L.A., Kobussen, A., 2016. Zircon compositions as a pathfinder for porphyry Cu ± Mo ± Au deposits. Econ. Geol. Spe. Publ. 19, 329–347.

Lupulescu, M.V., Chiarenzelli, J.R., Pullen, A.P., Price, J.D., 2011. Using pegmatite geochronology to constrain temporal events in the Adirondack Mountains. Geosphere 7, 23–39.

Maneta, V., Baker, D.R., Minarik, W., 2015. Evidence for lithium-aluminosilicate supersaturation of pegmatite-forming melts. Contrib. Mineral. Petrol. 170. https://doi.org/10.1007/s00410-015-1158-z.

Mangler, M., Gardiner, N.J., Roberts, N.M.W., Skeat, D., 2024. Apatite as an indicator mineral for tin and lithium mineralisation: challenges and opportunities. https://doi.org/10.31223/X5NX3R.

Manning, D.A.C., 1986. Contrasting styles of Sn-W mineralisation in peninsular Thailand and SW England. Mineral. Deposita 21. https://doi.org/10.1007/BF00204360.

Manning, D.A.C., Exley, C.S., 1984. The origins of late-stage rocks in the St Austell granite—a re-interpretation. J. Geol. Soc. Lond. 141, 581–591.

Mao, M., Rukhlov, A.S., Rowins, S.M., Spence, J., Coogan, L.A., 2016. Apatite trace element compositions: a robust new tool for mineral exploration. Econ. Geol. 111, 1187–1222.

Marignac, C., Cuney, M., 1999. Ore deposits of the French Massif Central: insight into the metallogenesis of the Variscan collision belt. Mineral. Deposita 34, 472–504.

Martins, T., Roda-Robles, E., Lima, A., De Parseval, P., 2012. Geochemistry and evolution of micas in the Barroso-Alvao pegmatite field, northern Portugal. Can. Mineral. 50, 1117–1129. https://doi.org/10.3749/canmin.50.4.1117.

McBride, S.L., Robertson, R.C.R., Clark, A.H., Farrar, E., 1983. Magmatic and Metallogenetic Episodes in the Northern Tin Belt, Cordillera real, Bolivia. Geol. Rundsch. 72, 685–713.

McCaffrey, D.M., Jowitt, S.M., 2023. The Crystallization Temperature of Granitic Pegmatites: the Important Relationship between Undercooling and critical Metal Prospectivity. Earth Sci. Rev. 244, 104541.

McCauley, A., Bradley, D.C., 2014. The global age distribution of granitic pegmatites. Can. Mineral. 52, 183–190.

McCuaig, T.C., Hronsky, J.M.A., 2014. The Mineral System Concept: the Key to Exploration Targeting. Econ. Geol. Spe. Publ. 18, 153–175.

McNulty, B., Jowitt, S., 2021. Barriers to and uncertainties in understanding and quantifying global critical mineral and element supply. iScience 23.

Melcher, F., Graupner, T., Gäbler, H.-E., Sitnikova, M., Henjes-Kunst, F., Oberthür, T., Gerdes, A., Dewaele, S., 2015. Tantalum–(niobium–tin) mineralisation in African pegmatites and rare metal granites: Constraints from Ta–Nb oxide mineralogy, geochemistry and U–Pb geochronology. Ore Geol. Rev. 64, 667–719. https://doi.org/10.1016/j.oregeorev.2013.09.003.

Miles, A.J., Graham, C.M., Hawkesworth, C.J., Gillespie, M.R., Hinton, R.W., Bromiley, G.D., 2014. Apatite: a new redox proxy for silicic magmas? Geochim. Cosmochim. Acta 132, 101–119. https://doi.org/10.1016/j.gca.2014.01.040.

Mitchell, A.H.G., 1977. Tectonic settings for emplacement of Southeast Asian tin granites. Bull. Geol. Soc. Malaysia 9, 123–140.

Mitchell, A.H.G., Garson, M.S., 1981. Mineral Deposits and Global Tectonic Settings. Academic Press, New York.

Mole, D.R., Fiorentini, M.L., Cassidy, K.F., Kirkland, C.L., Thebaud, N., McCuaig, T.C., Doublier, M.P., Duuring, P., Romano, S.S., Maas, R., Belousova, E.A., Barnes, S.J., Miller, J., 2015. Crustal evolution, intra-cratonic architecture and the metallogeny of an Archaean craton. Geol. Soc. Lond. Spec. Publ. 393, 23–80. https://doi.org/10.1144/sp393.8.

Mole, D.R., Kirkland, C.L., Fiorentini, M.L., Barnes, S.J., Cassidy, K.F., Isaac, C., Belousova, E.A., Hartnady, M., Thebaud, N., 2019. Time-space evolution of an Archean craton: a Hf-isotope window into continent formation. Earth Sci. Rev. 196. https://doi.org/10.1016/j.earscirev.2019.04.003.

Monnier, L., Salvi, S., Melleton, J., Lach, P., Pochon, A., Bailly, L., Béziat, D., De Parseval, P., 2022. Mica trace-element signatures: Highlighting superimposed W-Sn mineralizations and fluid sources. Chem. Geol. 600, 120866.

Montel, J.M., Vielzeuf, D., 1997. Partial melting of metagreywackes, Part II. Compositions of minerals and melts. Contrib. Mineral. Petrol. 128, 176–196.

Moretz, L., Heimann, A., Bitner, J., Wise, M., Rodrigues Soares, D., Mousinho Ferreira, A., 2013. The composition of garnet as indicator of rare metal (Li) mineralization in granitic pegmatites. In: Presented at the International Symposium on Granitic Pegmatites, pp. 94–95.

Morgan, G.B., London, D., 1987. Alteration of Amphibolitic Wallrocks around the Tanco Rare-Element Pegmatite, Bernic Lake, Manitoba. Am. Mineral. 72, 1097–1121.

Moyen, J.F., 2009. High Sr/Y and La/Yb Ratios: The Meaning of the "Adakitic Signature". Lithos 112, 556–574.

Moyen, J.F., 2020. Granites and crustal heat budget. Geol. Soc. Lond. Spec. Publ. 491, 77–100.

Moyen, J.-F., Martin, H., 2012. Forty years of TTG research. Lithos 148, 312–336. https://doi.org/10.1016/j.lithos.2012.06.010.

Müller, A., Romer, R., Pederson, R., 2017. The sveconorwegian pegmatite province -thousands of pegmatites without parental granites. Can. Mineral. 55, 283–315.

Müller, A., Keyser, W., Simmons, W.B., Webber, K.L., Wise, M., Beurlen, H., Garate-Olave, I., Roda Robles, E., Galliski, M.A., 2021. Quartz chemistry of granitic pegmatites: Implications for classification, genesis and exploration. Chem. Geol. 584, 120507.

Nardi, L.V.S., Formoso, M.L.L., Müller, I.F., Fontana, E., Jarvis, K., Lamarão, C., 2013. Zircon/rock partition coefficients of REEs, Y, Th, U, Nb, and Ta in granitic rocks: Uses for provenance and mineral exploration purposes. Chem. Geol. 335, 1–7. https://doi.org/10.1016/j.chemgeo.2012.10.043.

Naumov, V.B., Dorofeev, V.A., Mironova, O.F., 2011. Physicochemical parameters of the formation of hydrothermal deposits: a fluid inclusion study. I. Tin and tungsten deposits. Geochem. Int. 49, 1002–1021.
Norton, J., 1983. Sequence of Mineral Assemblages in Differentiated Granitic Pegmatites. Econ. Geol. 78, 854–874.
O'Sullivan, G.J., Chew, D.M., 2020. The clastic record of a Wilson Cycle: evidence from detrital apatite petrochronology of the Grampian-Taconic fore-arc. Earth Planet. Sci. Lett. 552, 116588.
Palin, R.M., White, R.W., Green, E.C.R., Diener, J.F.A., Powell, R., Holland, T.J.B., 2016. High-grade metamorphism and partial melting of basic and intermediate rocks. J. Metamorph. Geol. 34, 871–892. https://doi.org/10.1111/jmg.12212.
Partington, G.A., 2017. Greenbushes tin, tantalum and lithium deposit. In: Phillips, G.N. (Ed.), Australian Ore Deposits. The Australian Institute of Mining and Metallurgy, Melbourne, Australia, pp. 153–157.
Patiño-Douce, A.E., Johnston, A.D., 1991. Phase equilibria and melt productivity in the pelitic system: implications for the origin of peraluminous granitoids and aluminous granites. Contrib. Mineral. Petrol. 107, 202–218.
Pettke, T., Audétat, A., Schaltegger, U., Heinrich, C.A., 2005. Magmatic-to-hydrothermal crystallization in the W–Sn mineralized Mole Granite (NSW, Australia). Chem. Geol. 220, 191–213. https://doi.org/10.1016/j.chemgeo.2005.02.017.
Phelps, P.R., Lee, C.-T.A., Morton, D.M., 2020. Episodes of Fast Crystal Growth in Pegmatites. Nat. Commun. 11, 4986.
Phelps-Barber, Z., Trench, A., Groves, D., 2022. Recent pegmatite-hosted spodumene discoveries in Western Australia: insights for lithium exploration in Australia and globally. Appl. Earth Sci. 131, 100–113.
Plunder, A., Le Pourhlet, L., Räss, L., Gloaguen, E., Pichavant, M., Gumiaux, C., 2022. Pegmatites as geological expressions of spontaneous crustal flow localisation. Lithos 416–417, 106652.
Poli, S., Schmidt, M.W., 2002. Petrology of subducted slabs. Annu. Rev. Earth Planet. Sci. 30, 207–235.
Pollard, P.J., Taylor, R.G., 1986. Progressive evolution of alteration and tin mineralisation: Controls by interstitial permeability and fracture-related tapping of magmatic fluid reservoirs in tin granites. Econ. Geol. 81, 1795–1800.
Pollard, P.J., Pichavant, M., Charoy, B., 1987. Contrasting evolution of fluorine- and boron-rich tin systems. Mineral. Deposita 22, 315–321.
Popov, D., 2023. Do pegmatites crystallise fast? A perspective from petrologically-constrained isotopic dating. Geosciences 13, 297.
Powell, R., Holland, T.J.B., 2008. On thermobarometry. J. Metamorph. Geol. 26, 155–179.
Putzolu, F., Seltmann, R., Dolgopolova, D., Armstrong, R.A., Shail, R.K., Spratt, J., Buret, Y., Broderick, C., Brownscombe, W., 2024. Influence of magmatic and magmatic-hydrothermal processes on the lithium endowment of micas in the Cornubian Batholith (SW England). Mineral. Deposita 59, 1067–1088.
Raimbault, L., Cuney, M., Azencott, C., Duthou, J.-L., Joron, J.L., 1995. Geochemical evidence for a multistage magmatic genesis of Ta-Sn-Li mineralization in the granite at Beauvoir, French Massif Central. Econ. Geol. 90, 548–576. https://doi.org/10.2113/gsecongeo.90.3.548.
Redlinger, M., Eggert, R.D., 2016. Volatility of by-product metal and mineral prices. Res. Policy 47, 69–77.
Richards, J.P., 2011. Magmatic to hydrothermal metal fluxes in convergent and collided margins. Ore Geol. Rev. 40, 1–26. https://doi.org/10.1016/j.oregeorev.2011.05.006.
Robb, L.J., Robb, V.M., 1986. Archaean pegmatite deposits in the North Eastern Transvaal. In: Mineral Deposits of Southern Africa. Geological Society of South Africa, Johannesburg, pp. 437–449.
Robb, L.J., Freeman, L.A., Armstrong, R.A., 2000. Nature and longevity of hydrothermal fluid flow and mineralization in granites of the Bushveld Complex, South Africa. Trans. R. Soc. Edinb. Earth Sci. 91, 269–281.
Roberts, N.M.W., Spencer, C.J., 2015. The zircon archive of continent formation through time. Geol. Soc. Lond. Spec. Publ. 389, 197–225. https://doi.org/10.1144/sp389.14.
Roberts, N.M.W., Yakymchuk, C., Spencer, C.J., Keller, C.B., Tapster, S.R., 2024. Revisiting the discrimination and distribution of S-type granites from zircon trace element composition. Earth Planet. Sci. Lett. 633, 118638. https://doi.org/10.1016/j.epsl.2024.118638.
Roda Robles, E., Pesquera Perez, A., Velasco Roldan, F., Fontan, F., 1999. The granitic pegmatites of the Fregeneda area (Salamanca, Spain): characteristics and petrogenesis. Mineral. Mag. 63, 535–558.
Roda-Robles, E., Pesquera, A., Gil, P.P., Torres-Ruiz, J., Fontan, F., 2004. Tourmaline from the rare-element Pinilla pegmatite, (Central Iberian Zone, Zamora, Spain): chemical variation and implications for pegmatitic evolution. Mineral. Petrol. 81, 249–263.
Roda-Robles, E., Simmons, W.B., Pesquera, A., Gil-Crespo, P.P., Nizamoff, J., Torres-Ruiz, J., 2015. Tourmaline as a petrogenetic monitor of the origin and evolution of the Berry-Havey pegmatite (Maine, U.S.a.). Am. Mineral. 100, 95–109.
Romer, R.L., Kroner, U., 2015. Sediment and weathering control on the distribution of Paleozoic magmatic tin–tungsten mineralization. Mineral. Deposita 50, 327–338. https://doi.org/10.1007/s00126-014-0540-5.
Romer, R.L., Kroner, U., 2016. Phanerozoic tin and tungsten mineralization—Tectonic controls on the distribution of enriched protoliths and heat sources for crustal melting. Gondwana Res. 31, 60–95. https://doi.org/10.1016/j.gr.2015.11.002.
Romer, R.L., Lehmann, B., 1995. U-Pb columbite age of Neoproterozoic Ta-Nb mineralization in Burundi. Econ. Geol. 90, 2303–2309. https://doi.org/10.2113/gsecongeo.90.8.2303.
Romer, R.L., Smeds, S.-A., 1996. U-Pb Columbite Ages of Pegmatites from Sveconorwegian Terranes in Southwestern Sweden. Precambrian Res. 76, 15–30.
Romer, R.L., Wright, J.E., 1992. U-Pb dating of columbites: a geochronologic tool to date magmatism and ore deposits. Geochim. Cosmochim. Acta 56, 2137–2142.
Romer, R.L., Thomas, R., Stein, H.J., Rhede, D., 2007. Dating multiply overprinted Sn-mineralized granites—examples from the Erzgebirge, Germany. Mineral. Deposita 42, 337–359.
Romer, R.L., Meixner, A., Förster, H.-J., 2014. Lithium and boron in late-orogenic granites – Isotopic fingerprints for the source of crustal melts? Geochim. Cosmochim. Acta 131, 98–114. https://doi.org/10.1016/j.gca.2014.01.018.
Rosenberg, C.L., Handy, M.R., 2005. Experimental deformation of partially melted granite revisited: implications for the continental crust. J. Metamorph. Geol. 23, 19–28. https://doi.org/10.1111/j.1525-1314.2005.00555.x.
Rudnick, R.L., Gao, S., 2014. Composition of the Continental Crust. Treatise on. Geochemistry 1–51. https://doi.org/10.1016/b978-0-08-095975-7.00301-6, 2nd edition.
Ryabchikov, I.D., Durasova, N.A., Barsukov, V.I., Laputina, I.P., Afimov, A.S., 1978. Role of volatiles for the mobilization of tin from granitic magmas. In: Stemprok, M., Burnol, L., Tischendorf, B. (Eds.), Metallization Associated with Acid Magmatism. Czechoslovakia Geological Survey, Prague, pp. 94–109.
Scherer, E.E., Whitehouse, M., Munker, C., 2007. Zircon as a Monitor of Crustal Growth. Elements 3, 19–24.
Schmidt, C., Romer, R.L., Wohlgemuth-Ueberwasser, C.C., Appelt, O., 2020. Partitioning of Sn and W between granitic melt and aqueous fluid. Ore Geol. Rev. 117. https://doi.org/10.1016/j.oregeorev.2019.103263.
Schuiling, R.D., 1967. Tin belts on the continents around the Atlantic Ocean. Econ. Geol. 62, 540–550.
Schwartz, M.O., Rajah, S.S., Askury, A.K., Putthapiban, P., Djaswadi, S., 1995. The Southeast Asian Tin Belt. Earth Sci. Rev. 38, 95–293. https://doi.org/10.1016/0012-8252(95)00004-T.
Scrivener, R.C., 2006. Cornubian granites and mineralization of SW England. In: Brenchley, P.J., Rawson, P.F. (Eds.), The Geology of England and Wales. The Geological Society, London, UK.
Searle, M.P., Whitehouse, M.J., Robb, L.J., Ghani, A.A., Hutchison, C.S., Sone, M., Ng, S. W.P., Roselee, M.H., Chung, S.L., Oliver, G.J.H., 2012. Tectonic evolution of the Sibumasu-Indochina terrane collision zone in Thailand and Malaysia: constraints from new U-Pb zircon chronology of SE Asian tin granitoids. J. Geol. Soc. Lond. 169, 489–500. https://doi.org/10.1144/0016-76492011-107.
Sha, L.-K., Chappell, B.W., 1999. Apatite chemical composition, determined by electron microprobe and laser-ablation inductively coupled plasma mass spectrometry, as a probe into granite petrogenesis. Geochim. Cosmochim. Acta 63, 3861–3881.
Shail, R.K., Stuart, F.M., Wilkinson, J.J., Boyce, A.J., 2003. The role of post-Variscan extensional tectonics and mantle melting in the generation of the lower Permian granites and the giant W-As-Sn-Cu-Zn-Pb orefield of SW England. Appl. Earth Sci. 112, 127–129.
Shaw, R.A., Goodenough, K.M., Roberts, N.M.W., Horstwood, M.S.A., Chenery, S.R., Gunn, A.G., 2016. Petrogenesis of rare-metal pegmatites in high-grade metamorphic terranes: a case study from the Lewisian Gneiss complex of north-West Scotland. Precambrian Res. 281, 338–362. https://doi.org/10.1016/j.precamres.2016.06.008.
Shaw, R.A., Goodenough, K.M., Deady, E., Nex, P., Ruzvidzo, B., Rushton, J.C., Mounteney, I., 2022. The magmatic–hydrothermal transition in lithium pegmatites: petrographic and geochemical characteristics of pegmatites from the Kamativi Area, Zimbabwe. Can. Mineral. 60, 957–987. https://doi.org/10.3749/canmin.2100032.
Sillitoe, R.H., 2010. Porphyry Copper Systems. Econ. Geol. 105, 3–41.
Silva, D., Groat, L.A., Martins, T., Linnen, R.L., 2023. Structural controls on the origin and emplacement of lithium-bearing pegmatites. Can. J. Min. Petrol. 61, 1053–1062.
Simmons, W.B., Webber, K.L., 2008. Pegmatite Genesis: State of the Art. Eur. J. Mineral. 20, 421–438.
Simmons, W.B., Foord, E.E., Falster, A.U., King, V.T., 1995. Evidence for an Anatectic Origin of Granitic Pegmatites, Western Maine. Presented at the Geological Society of America Annual Meeting, New Orleans, USA.
Simons, B., Shail, R.K., Andersen, J.C.Ø., 2016. The petrogenesis of the early Permian Variscan granites of the Cornubian Batholith: lower plate post-collisional peraluminous magmatism in the Rhenohercynian Zone of SW England. Lithos 260, 76–94. https://doi.org/10.1016/j.lithos.2016.05.010.
Simons, B., Andersen, J.C.Ø., Shail, R.K., Jenner, F.E., 2017. Fractionation of Li, Be, Ga, Nb, Ta, In, Sn, Sb, W and Bi in the peraluminous Early Permian Variscan granites of the Cornubian Batholith: Precursor processes to magmatic-hydrothermal mineralisation. Lithos 278–281, 491–512. https://doi.org/10.1016/j.lithos.2017.02.007.
Sirbescu, M.-L.C., Hartwick, E.E., Student, J.J., 2008. Rapid Crystallization of the Animikie Red Ace Pegmatite, Florence County, Northeastern Wisconsin: Inclusion Microthermometry and Conductive-Cooling Modeling. Contrib. Mineral. Petrol. 156, 289–305.
Smith, D.J., Wentworth, J., 2022. Mining and the Sustainability of Metals. Parliamentary Office of Science and Technology, UK Parliament, London.
Smith, S.R., Foster, G.L., Romer, R.L., Tindle, A., Kelley, S., Noble, S.R., Horstwood, M.S. A., Breaks, F.W., 2004. U-Pb columbite-tantalite chronology of rare-element pegmatites using TIMS and laser ablation-multi collector-ICP-MS. Contrib. Mineral. Petrol. 147, 549–564.
Spear, F.S., Kohn, M.J., Cheney, J.T., 1999. P-T paths from anatectic pelites. Contrib. Mineral. Petrol. 134, 17–32.
Starkey, H.C., 1982. The Role of Clays in Fixing Lithium. USGS Bulletin 1278-F.
Stewart, D.B., 1978. Petrogenesis of lithium-rich pegmatites. Am. Mineral. 63, 970–980.
Stilling, A.P., Cerny, P., Vanstone, P.J., 2006. The Tanco pegmatite at Bernic Lake, Manitoba. XVI. Zonal and Bulk Compositions and their petrogenetic significance. Can. Mineral. 44, 599–623.

Stock, M.J., Humphreys, M.C.S., Smith, V.C., Isaia, R., Pyle, D.M., 2016. Late-stage volatile saturation as a potential trigger for explosive volcanic eruptions. Nat. Geosci. 9, 249–254. https://doi.org/10.1038/ngeo2639.
Strong, D.F., 1981. Ore Deposit Models - 5. A model for granophile mineral deposits. Geosci. Can. 8, 155–161.
Sun, K.-K., She, J.-X., Du, D.-H., Li, W., Deng, J., 2024. Extreme Sn isotope fractionation in highly evolved granites. Chem. Geol. 664, 121843.
Suwimonprecha, P., Cerny, P., Friedrich, G., 1995. Rare Metal Mineralization Related to Granites and Pegmatites, Phuket, Thailand. Econ. Geol. 90, 603–615.
Swanson, S.E., 2012. Mineralogy of spodumene pegmatites and related rocks in the tin-spodumene belt of North Carolina and South Carolina, USA. Can. Mineral. 50, 1589–1608.
Sweetapple, M.T., 2017a. A review of the setting and internal characteristics of lithium pegmatite systems of the Archaean North Pilbara and Yilgarn Cratons, Western Australia. In: Presented at the Granites 2017, Ext Abstr Austr Inst Geosci Bull. Benalla, Victoria, Australia.
Sweetapple, M.T., 2017b. Granitic pegmatites as mineral systems: examples from the Archaean. In: NGF Abstracts and Proceedings, pp. 139–142.
Sweetapple, M.T., Collins, W.J., 2002. Genetic framework for the classification and distribution of Archean rare metal pegmatites in the North Pilbara Craton, Western Australia. Econ. Geol. 97, 873–895.
Sweetapple, M.T., Grigson, M.W., Tornatora, P., Urgine, S., 2019. The Archean Mt. Cattlin Spodumene Pegmatite Group and 3D Geochemical Mapping of large 'unzoned' Pegmatites of Economic significance. Can. Mineral. 57, 803–805.
Tapster, S., Bright, J.W.G., 2020. High-precision ID-TIMS cassiterite U–Pb systematics using a low-contamination hydrothermal decomposition: implications for LA-ICP-MS and ore deposit geochronology. Geochronology 2, 425–441. https://doi.org/10.5194/gchron-2-425-2020.
Tavazzani, L., Wotzlaw, J.-F., Economos, R., Sinigoi, S., Demarchi, G., Szymanowski, D., Laurent, O., Bachmann, O., Chelle-Michou, C., 2023. High-precision zircon age spectra record the dynamics and evolution of large open-system silicic magma reservoirs. Earth Planet. Sci. Lett. 623, 118432. https://doi.org/10.1016/j.epsl.2023.118432.
Taylor, R.G., 1979. Geology of Tin Deposits, Developments in Economic Geology. Elsevier, Amsterdam.
Taylor, J.R., Wall, V.J., 1992. The behaviour of tin in granitoid magmas. Econ. Geol. 87, 403–420.
Teng, Z.-T., Li, W.-Y., Rudnick, R.L., Gardiner, L.R., 2010. Contrasting lithium and magnesium isotope fractionation during continental weathering. Earth Planet. Sci. Lett. 300, 63–71.
Tindle, A., Breaks, F., 2000. Columbite-tantalite mineral chemistry from rare-element granitic pegmatites: Separation Lakeh area, N.W. Ontario, Canada. Mineral. Petrol. 70, 165–198.
Tinto, Rio, Latham, A., 2018. Rio Tinto Ventures and Rio Tinto's Jadar Project.
Tkachev, A.V., 2011. Evolution of metallogeny of granitic pegmatites associated with orogens throughout geological time. In: Sial, A.N., Bettencourt, J.S., De Campos, C. P., Ferreira, V.P. (Eds.), Granite-Related Ore Deposits. The Geological Society, pp. 7–23.
Tomascak, P., Krogstad, E.J., Walker, R., 1998. Sm-Nd Isotope systematics and the derivation of granitic pegmatites in southwestern Maine. Can. Mineral. 36, 327–337.
Trail, D., Chowdhury, W., Tailby, N.D., Ackerson, M., 2024. Ce and Eu anomalies in zircon as indicators of oxygen fugacity in subsolidus systems. Geochim. Cosmochim. Acta 369, 93–110. https://doi.org/10.1016/j.gca.2024.01.024.
Troch, J., Huber, C., Bachmann, O., 2022. The physical and chemical evolution of magmatic fluids in near-solidus silicic magma reservoirs: Implications for the formation of pegmatites. Am. Mineral. 107, 190–205. https://doi.org/10.2138/am-2021-7915.
Trumbull, R.B., 1993. A petrological and Rb-Sr isotopic study of an early Archean fertile granite-pegmatite system: the Sinceni Pluton in Swaziland. Precambrian Res. 61, 89–116. https://doi.org/10.1016/0301-9268(93)90059-B.
Turneaure, F.S., 1971. Bolivian tin-silver province. Econ. Geol. 66, 215–225.
US Geological Survey, 2023. Mineral Commodity Summaries 2023. United States Geological Survey.
Valley, J., 2003. Oxygen Isotopes in Zircon. Rev. Mineral. Geochem. 53, 343–385.
Vielzeuf, D., Holloway, J., 1988. Experimental determination of the fluid-absent melting relations in the pelitic system: consequences for crustal differentiation. Contrib. Mineral. Petrol. 98, 257–276.
Vigneresse, J.L., Barbey, P., Cuney, M., 1996. Rheological transitions during partial melting and crystallization with application to felsic magma segregation and transfer. J. Petrol. 37, 1579–1600.
Walshe, J.L., Solomon, M., Whitford, D.J., Sun, S.-S., Foden, J.D., 2011. The role of the mantle in the genesis of tin deposits and tin provinces of Eastern Australia. Econ. Geol. 106, 297–305. https://doi.org/10.2113/econgeo.106.2.297.
Wang, C., Shao, Y.J., Cawood, P.A., Chen, J.F., Xiong, Y.Q., Wang, Y.J., 2023. Regional zoning of a Li-Cs-Ta pegmatite field: Insights from monazite-cheralite chemistry, U-Th-Pb and Sm-Nd isotopes. J. Petrol. 64, egad044.
Webber, K.L., Simmons, W.B., Falster, A.U., Foord, E.E., 1999. Cooling rates and Crystallization Dynamics of Shallow Level Pegmatite-Aplite Dikes, San Diego County, California. Am. Mineral. 84, 708–717.
Werner, A.G., 1791. Neue Theorie Von Der Entstehung Der Gänge: Mit Anwendung Auf Den Bergbau Besonders Den Freibergischen. Gerlachische Buchdruckerei, Freiberg.
White, R.W., Powell, R., Holland, T.J.B., 2007. Progress relating to calculation of partial melting equilibria for metapelites. J. Metamorph. Geol. 25, 511–527.
White, R.W., Powell, R., Holland, T.J.B., Johnson, T.E., Green, E.C.R., 2014. New mineral activity-composition relations for thermodynamic calculations in metapelitic systems. J. Metamorph. Geol. 32, 261–286. https://doi.org/10.1111/jmg.12071.
Whitney, J.A., Naldrett, A.J., 1989. Ore Deposition Associated with Magmas, Reviews in Economic Geology. Society of Economic Geologists.
Wilde, A., Otto, A., McCracken, S., 2021. Geology of the Goulamina Spodumene Pegmatite Field, Mali. Ore Geol. Rev. 134, 104162.
Williamson, B.J., Herrington, R.J., Morris, A., 2016. Porphyry copper enrichment linked to excess aluminium in plagioclase. Nat. Geosci. 9, 237–241. https://doi.org/10.1038/ngeo2651.
Wise, M.A., Cerny, P., 1990. Primary Compositional Range and Alteration Trends of Microlite from the Yellowknife Pegmatite Field, Northwest Territories, Canada. Mineral. Petrol. 43, 83–98.
Wolf, M., Romer, R.L., Franz, L., López-Moro, F.J., 2018. Tin in granitic melts: the role of melting temperature and protolith composition. Lithos 310–311, 20–30. https://doi.org/10.1016/j.lithos.2018.04.004.
Wood, S.A., 2005. The aqueous geochemistry of zirconium, hafnium, niobium and tantalum. Geol. Assoc. Can. Short Course Notes 17, 217–250.
Wyborn, D., Heinrich, C.A., Jaques, A.L., 1994. Australian Proterozoic Mineral Systems; Essential Ingredients and Mappable Criteria. Presented at the AusIMM Annual Conference. AusIMM, pp. 109–115.
Yakymchuk, C., Holder, R.M., Kendrick, J., Moyen, J.F., 2023. Europium anomalies in zircon: a signal of crustal depth? Earth Planet. Sci. Lett. 622, 118405.
Zack, T., Hogmalm, K.J., 2016. Laser ablation Rb/Sr dating by online chemical separation of Rb and Sr in an oxygen-filled reaction cell. Chem. Geol. 437, 120–133. https://doi.org/10.1016/j.chemgeo.2016.05.027.
Zaw, Khin, 1990. Geological, petrological and geochemical characteristics of granitoid rocks in Burma: with special reference to the associated W-Sn mineralization and their tectonic setting. J. SE Asian Earth Sci. 4, 293–335.
Zhang, H., Tian, S., Wang, D., Li, X., Liu, T., Zhang, Y., Fu, X., Hao, X., Hou, K., Zhao, Y., Qin, Y., 2021. Lithium isotope behavior during magmatic differentiation and fluid exsolution in the Jiajika granite–pegmatite deposit, Sichuan, China. Ore Geol. Rev. 134, 104139.
Zhao, P., Chu, X., Williams-Jones, A.E., Mao, J., Yuan, S., 2022a. The role of phyllosilicate partial melting in segregating tungsten and tin deposits in W-Sn metallogenic provinces. Geology 50, 121–125. https://doi.org/10.1130/g49248.1.
Zhao, P., Zajacz, Z., Tsay, A., Yuan, S., 2022b. Magmatic-hydrothermal tin deposits form in response to efficient tin extraction upon magma degassing. Geochim. Cosmochim. Acta 316, 331–346. https://doi.org/10.1016/j.gca.2021.09.011.